

Three years of Ulysses dust data: 2005 to 2007

H. Krüger^{a,b,1}, V. Dikarev^c, B. Anweiler^b, S. F. Dermott^d, A. L. Graps^e, E. Grün^{b,f},
 B. A. Gustafson^d, D. P. Hamilton^g, M. S. Hanner^h, M. Horányi^f, J. Kissel^a, D. Linkert^b,
 G. Linkert^b, I. Mannⁱ, J. A. M. McDonnell^j, G. E. Morfill^k, C. Polansky^l, G. Schwehm^m
 and R. Srama^{b,n}

- a) Max-Planck-Institut für Sonnensystemforschung, 37191 Katlenburg-Lindau, Germany
- b) Max-Planck-Institut für Kernphysik, 69029 Heidelberg, Germany
- c) Fakultät für Physik, Universität Bielefeld, Postfach 100131, 33501 Bielefeld, Germany
- d) University of Florida, 211 SSRB, Campus, Gainesville, FL 32609, USA
- e) Department of Space Studies, Southwest Research Institute, 1050 Walnut Street Suite 300, Boulder, Colorado, 80302, USA
- f) Laboratory for Atmospheric and Space Physics, Univ. of Colorado, Boulder, CO 80309, USA
- g) University of Maryland, College Park, MD 20742-2421, USA
- h) Astronomy Dept. 619 LGRT, University of Massachusetts, Amherst MA 01003, USA
- i) School of Science and Engineering, Kindai University, Kowakae 3-4-1, Higashi-Osaka, Osaka, 577-8502, Japan
- j) Planetary and Space Science Research Institute, The Open University, Milton Keynes, MK7 6AA, UK
- k) Max-Planck-Institut für Extraterrestrische Physik, 85748 Garching, Germany
- l) Jet Propulsion Laboratory, Pasadena, California 91109, USA
- m) ESAC, PO Box 78, 28691 Villanueva de la Cañada, Spain
- n) Universität Stuttgart, Institut für Raumfahrtssysteme, Pfaffenwaldring 31, 70569 Stuttgart, Germany

Abstract

The Ulysses spacecraft has been orbiting the Sun on a highly inclined ellipse ($i = 79^\circ$, perihelion distance 1.3 AU, aphelion distance 5.4 AU) since it encountered Jupiter in February 1992. Since then it made almost three revolutions about the Sun. Here we report on the final three years of data taken by the on-board dust detector. During this time, the dust detector recorded 609 dust impacts of particles with masses $10^{-16} \text{ g} \leq m \leq 10^{-7} \text{ g}$, bringing the mission total to 6719 dust data sets. The impact rate varied from a low value of 0.3 per day at high ecliptic latitudes to 1.5 per day in the inner solar system. The impact direction of the majority of impacts between 2005 and 2007 is compatible with particles of interstellar origin, the rest are most likely interplanetary particles. We compare the interstellar dust measurements from 2005/2006 with the data obtained during earlier periods (1993/1994) and (1999/2000) when Ulysses was traversing the same spatial region at southern ecliptic latitudes but the solar cycle was at a different phase. During these three intervals the impact rate of interstellar grains varied by more than a factor of two. Furthermore, in the two earlier periods the grain

¹Correspondence to: Harald Krüger, krueger@mps.mpg.de

22 impact direction was in agreement with the flow direction of the interstellar helium
23 while in 2005/2006 we observed a shift in the approach direction of the grains by
24 approximately 30° away from the ecliptic plane. The reason for this shift remains
25 unclear but may be connected with the configuration of the interplanetary magnetic
26 field during solar maximum. We also find that the dust measurements are in agreement
27 with the interplanetary flux model of Staubach et al. (1997) which was developed to
28 fit a 5-year span of Ulysses data.

29 **1 Introduction**

30 Ulysses was the only space mission so far that left the ecliptic plane and flew over the poles
31 of the Sun. The spacecraft was launched in 1990 and was very successfully operated un-
32 til 30 June 2009, although individual instruments had to be turned off to conserve power.
33 Its orbital plane was almost perpendicular to the ecliptic plane (79° inclination) with an
34 aphelion at Jupiter. This special orbit orientation allowed Ulysses to unambiguously detect
35 interstellar dust grains entering the heliosphere because the spacecraft's orbital plane was
36 almost perpendicular to the flow direction of the interstellar dust. Ulysses had a highly
37 sensitive impact ionisation dust detector on board which measured impacts of micrometre
38 and sub-micrometre dust grains. The detector was practically identical with the dust in-
39 strument which flew on board the Galileo spaceprobe. Both instruments were described in
40 previous publications by Grün et al. (1992a,b, 1995c).

41 **1.1 Summary of results from the Ulysses dust investigations**

42 Comprehensive reviews of the scientific achievements of the Ulysses mission including
43 results from the dust investigation were given by Balogh et al. (2001) and Grün et al.
44 (2001). References to other works related to Ulysses and Galileo measurements on dust
45 in the planetary system were also given by Grün et al. (1995a,b); Krüger et al. (1999a,b,
46 2001a,b, 2006b,a); Krüger and Grün (2009). Some mission highlights are also summarized
47 in Table 1.

48 Various dust populations were investigated with the Ulysses and Galileo dust experiments
49 in interplanetary space: the interplanetary dust complex including β -meteoroids (i.e. dust
50 particles which leave the solar system on unbound orbits due to acceleration by radiation
51 pressure), interstellar grains sweeping through the heliosphere, and dust stream particles
52 expelled from the jovian system by electromagnetic forces, to name only the most signif-
53 icant dust types detected with Ulysses which have been analysed so far. In the following,
54 we summarise the most significant achievements of the Ulysses dust measurements.

55 Ulysses and Galileo dust measurements were used to study the 3-dimensional structure
56 of the interplanetary dust complex and its relation to the underlying populations of parent
57 bodies like asteroids and comets (Divine, 1993; Grün et al., 1997; Staubach et al., 1997).
58 Studies of asteroidal dust released from the IRAS dust bands show that they are not efficient

59 enough dust sources to maintain the observed interplanetary dust cloud (Mann et al., 1996).
60 The state of the inner solar system dust cloud within approximately 1 AU from the Sun in-
61 cluding dust destruction and ion formation processes in relation to so-called solar wind
62 pickup ions detected by the Solar Wind Ion Composition Spectrometer (SWICS) onboard
63 Ulysses was investigated (Mann et al., 2004; Mann and Czechowski, 2005). An improved
64 physical model was developed for the interplanetary meteoroid environment (Dikarev et al.,
65 2001, 2002, 2005) which uses long-term particle dynamics to define individual interplane-
66 tary dust populations. The Ulysses and Galileo in-situ dust data are an important data set
67 for the validation of this model. The properties of β -meteoroids were also studied with
68 the Ulysses data set (Wehry and Mann, 1999; Wehry et al., 2004). Finally, the potential
69 connection of cometary dust trails and enhancements of the interplanetary magnetic field
70 as measured by Ulysses was discussed by Jones and Balogh (2003).

71 During its first flyby at Jupiter in 1992, the Ulysses dust instrument discovered burst-like
72 intermittent streams of tiny dust grains in interplanetary space (Grün et al., 1993) which
73 had been emitted from the jovian system (Hamilton and Burns, 1993; Horányi et al., 1993;
74 Zook et al., 1996). This discovery was completely unexpected as no periodic phenomenon
75 for tiny dust grains in interplanetary space was previously known. These grains strongly
76 interacted with the interplanetary and the jovian magnetic fields (Horányi et al., 1997;
77 Grün et al., 1998) and the majority of them originated from Jupiter's moon Io (Graps et al.,
78 2000). In February 2004 Ulysses had its second Jupiter flyby (at 0.8 AU distance from the
79 planet) and again measured the jovian dust streams (Krüger et al., 2005a, 2006c; Flandes
80 and Krüger, 2007; Flandes et al., 2009).

81 Another important discovery made with Ulysses were interstellar dust particles sweeping
82 through the heliosphere (Grün et al., 1993). The grains which originated from the very
83 local interstellar environment of our solar system were identified by their impact direction
84 and impact velocities, the latter being compatible with particles moving on hyperbolic
85 heliocentric trajectories (Grün et al., 1994). Their dynamics depends on the grain size
86 and is strongly affected by the interaction with the interplanetary magnetic field and by
87 solar radiation pressure (Landgraf et al., 1999; Landgraf, 2000; Mann and Kimura, 2000;
88 Czechowski and Mann, 2003b,a; Landgraf et al., 2003). As a result, the size distribution
89 and fluxes of grains measured inside the heliosphere are strongly modified. Studies of
90 the dust impacts detected with both Ulysses and Galileo showed that the intrinsic size
91 distribution of interstellar grains in the local interstellar environment of our solar system
92 extends to grain sizes larger than those detectable by astronomical observations (Frisch
93 et al., 1999; Frisch and Slavin, 2003; Landgraf et al., 2000; Grün and Landgraf, 2000).
94 Observations of radar meteors entering the Earth's atmosphere at high speeds also indicate
95 the existence of even larger interstellar grains (Taylor et al., 1996; Baggaley and Neslušan,
96 2002).

97 The Ulysses and Galileo interstellar dust measurements showed that the dust-to-gas mass
98 ratio in the local interstellar cloud is higher than the standard interstellar value derived
99 from cosmic abundances (Landgraf, 1998; Frisch et al., 1999). This implied the existence
100 of inhomogeneities in the diffuse interstellar medium on relatively small length scales. In

101 2005/2006 the Ulysses measurements showed a 30° shift in the impact direction of inter-
102 stellar grains with respect to the interstellar helium flow (Krüger et al., 2007). The reason
103 of this shift is presently unclear. Finally, it turned out that the dust sensor side walls have a
104 similar sensitivity to dust impacts as the detector target itself (Altobelli et al., 2004; Willis
105 et al., 2005). This shows that earlier investigations which neglected the contributions of
106 the side wall overestimated the interstellar dust flux by about 20%. Since the contribution
107 of the sensor side wall increases the effective dust instrument field-of-view, the velocity
108 dispersion of the observed interstellar dust stream turned out to be smaller by about 30%
109 than previously thought (Altobelli et al., 2004).

110 Due to its unique highly inclined heliocentric trajectory Ulysses was able to monitor in-
111 terstellar dust at high ecliptic latitudes between 3 and 5 AU. Dust measurements between
112 0.3 and 3 AU in the ecliptic plane exist also from Helios, Galileo and Cassini. This data
113 shows evidence for distance-dependent alteration of the interstellar dust stream caused by
114 radiation pressure, gravitational focussing and electromagnetic interaction of the grains with
115 the time-varying interplanetary magnetic field (Altobelli et al., 2003, 2005b,a).

116 **1.2 The Ulysses and Galileo dust data papers**

117 The Ulysses dust detector obtained dust data for more than 17 years, making it the longest
118 continually-operating spaceborne dust detector to date. With the publication of this paper,
119 the full Ulysses data set, along with 13 years of Galileo data, will be fully described in the
120 scientific literature. The reduction process of Ulysses and Galileo dust data was described
121 by Grün et al. (1995c, hereafter Paper I). In the odd-numbered Papers III, V, VII and IX
122 (Grün et al., 1995a; Krüger et al., 1999b, 2001b, 2006a) we presented the Ulysses data set
123 spanning the time period from launch in October 1990 to December 2004. The companion
124 even-numbered Papers II, IV, VI and VIII (Grün et al., 1995b; Krüger et al., 1999a, 2001a,
125 2006b) discussed the ten years of Galileo data from October 1989 to December 1999. The
126 current paper (Paper XI) extends the Ulysses data set from January 2005 until the Ulysses
127 dust measurements ceased in November 2007, and a companion paper (Krüger et al., 2010,
128 Paper X) presents Galileo's final measurements at Jupiter from 2000 to 2003. A summary
129 of the temporal and spatial coverage of our Ulysses data papers is given in Table 1.

130 The main data products are a table of the impact rate of all impacts determined from the par-
131 ticle accumulators and a table of both raw and reduced data of all dust impacts for which the
132 full data set of measured impact parameters was transmitted to Earth. The information pre-
133 sented in these papers is similar to data which we have submitted to the various data archiving
134 centres (Planetary Data System, NSSDC, Ulysses Data Centre). Electronic access to
135 the data is also possible via the world wide web: <http://www.mpi-hd.mpg.de/dustgroup/>.

136 This paper is organised like our earlier Papers III, V, VII and IX. We begin with an overview
137 of important events of the Ulysses mission between 2005 and 2007 (Section 2). Sections 3
138 and 4 describe and analyse the Ulysses dust data set for this period. In Section 5 we discuss
139 the dust data set from the entire Ulysses mission, we analyse in particular the interstellar
140 dust measurements obtained in the 2005 to 2007 interval, and we compare these results to

141 previous ones. In Section 6 we summarise our conclusions.

142 **2 Mission and instrument operation**

143 **2.1 Ulysses mission and dust instrument characteristics**

144 The Ulysses spacecraft was launched on 6 October 1990. A swing-by manoeuvre at Jupiter
145 in February 1992 rotated the orbital plane 79° relative to the ecliptic plane. On the resulting
146 trajectory (Figure 1) Ulysses finished two full revolutions about the Sun. Passages over
147 the south pole of the Sun occurred in October 1994, November 2000 and February 2007,
148 passages through the ecliptic plane at a perihelion distance of 1.3 AU occurred in March
149 1995, May 2001 and August 2007, and passes over the Sun's north pole were in August
150 1995, October 2001 and January 2008. In April 1998 and July 2004 the spacecraft crossed
151 the ecliptic plane at an aphelion distance of 5.4 AU. Orbital elements for the out-of-ecliptic
152 part of the Ulysses trajectory are given in Paper VII. Figure 1 shows that during most of
153 the time interval considered in this paper Ulysses was at southern ecliptic latitudes.

154 Ulysses is a spinning spacecraft, and the dust sensor orientation at the time of a dust par-
155 ticle impact is recorded, allowing for an independent determination of the grain impact
156 direction. Ulysses spins at five revolutions per minute about the centre line of its high
157 gain antenna which normally points at Earth. Figure 2 shows the deviation of the spin
158 axis from the Earth direction for the period 2005 to 2007. Most of the time the spin axis
159 pointing was within 1° of the nominal Earth direction, similar to the mission before 2005.
160 This small deviation is usually negligible for the analysis of measurements with the dust
161 detector. The Ulysses spacecraft and mission are explained in more detail by Wenzel et al.
162 (1992). Details about the data transmission to Earth can also be found in Paper III.

163 The Ulysses dust detector (GRU) has a 140° wide field of view and is mounted at the
164 spacecraft nearly at right angles (85°) to the antenna axis (spacecraft spin axis). Due to
165 this mounting geometry, the dust sensor is most sensitive to particles approaching from
166 the plane perpendicular to the spacecraft-Earth direction. The impact direction of dust
167 particles is measured by the rotation angle which is the sensor viewing direction at the
168 time of a dust impact. During one spin revolution of the spacecraft the rotation angle
169 scans through a complete circle of 360° . Zero degrees rotation angle is defined to be the
170 direction closest to ecliptic north. At high ecliptic latitudes, however, the sensor pointing at
171 0° rotation angle significantly deviates from the actual north direction. During the passages
172 over the Sun's polar regions the sensor always scans through a plane tilted by about 30°
173 from the ecliptic plane and all rotation angles lie close to the ecliptic plane (cf. Figure 4
174 in Grün et al., 1997). A sketch of the viewing geometry around aphelion passage can be
175 found in Grün et al. (1993).

176 The available electrical power on board Ulysses became an issue beginning in 2001 due
177 to decreasing power generation of the radioisotope batteries (RTGs). Some instrument
178 heaters on board had to be switched off to save power which in turn also reduced the on

179 board temperature. Later, in 2002, power consumption could not be sufficiently reduced
180 anymore by simply switching off heaters, and a cycling instrument operation scheme had
181 to be implemented: one or more of the scientific instruments had to be switched off at a
182 time. In the 2005 to 2007 interval considered in this paper the dust instrument was switched
183 off during a total time period of about seven months, separated into three individual time
184 periods (see Sect. 2.2). After 30 November 2007 the dust instrument remained switched
185 off permanently. It was planned to switch the dust instrument on in January 2008 again,
186 but due to a failure on board the spacecraft, this did not happen. Hence, no dust data were
187 obtained after 30 November 2007 although operation of the Ulysses spacecraft continued
188 until 30 June 2009.

189 **2.2 Dust instrument operation**

190 Table 2 gives significant mission and dust instrument events from 2005 to 2007. Earlier
191 events are only listed if especially significant. A comprehensive list of events from launch
192 until the end of 2004 was given in Papers III, V, VII and IX.

193 During the earlier Ulysses mission phases until 2000, several spacecraft anomalies oc-
194 curred during which all scientific instruments on board were switched off automatically
195 (Disconnection of all Non-Essential Loads – DNELs for short). No such anomaly occurred
196 in the 2005 to 2007 interval. The dust instrument was switched off between 28 September
197 2006 and 9 March 2007, from 2 April 2007 to 30 April 2007 and after 30 November 2007
198 (*cf.* Table 1), respectively, because there was not enough electrical power generated by the
199 RTGs anymore to operate all instruments simultaneously.

200 The dust instrument has two heaters to allow for a relatively stable operating temperature
201 within the sensor. By heating one of the two or both heaters, three different heating power
202 levels can be achieved (0.4 W, 0.8 W or 1.2 W; for comparison, the total power consump-
203 tion of the instrument without heaters is 2.2 W). Sensor heating was necessary when the
204 spacecraft was outside about 2 AU because relatively little radiation was received from the
205 Sun.

206 Before 2001 one or both heaters were switched on beyond 2 AU, except close to the Sun
207 when both were switched off. Since November 2001 the maximum allowed heating power
208 for nominal dust instrument operation has been limited to 0.8 W to save power on board
209 Ulysses. This reduced the sensor temperature by about 10° C as compared to the config-
210 uration with 1.2 W heating power at similar heliocentric distance. The full heating power
211 was only allowed for short periods before instrument switch on to avoid damage of the
212 electronics. In 2005 and 2006 the instrument was operated with 0.8 W heating power, and
213 in 2007 the heating power was set to 0.4 W, except during switch-ons when it was raised
214 to 1.2 W.

215 Table 2 lists the total powers consumed by the heaters. From 2005 to 2007 the temperature
216 of the dust sensor was between -37°C and $+16^{\circ}\text{C}$. The lower limit for the specified oper-
217 ational range is -30°C . No major effect of the reduced temperature was recognised (for an

218 anomalous temperature-related flipping in the housekeeping value of the channeltron high
219 voltage in 2004 see Paper IX).

220 No reprogramming of the Ulysses dust instrument occurred in the 2005 to 2007 interval.
221 In the earlier mission the instrument was reprogrammed three times and the reader is re-
222 ferred to Papers V and IX for details. In particular, a new classification scheme for impact
223 events was implemented in April 2002 which is the same as the one installed in the Galileo
224 instrument in July 1994 (Paper IV).

225 **2.3 Instrument sensitivity and noise**

226 Analysis of the in-orbit noise characteristics of the dust instrument (Paper III) led to a
227 relatively noise-free configuration with which the instrument was normally operated until
228 August 2000: channeltron voltage 1140 V (HV = 3); event definition status such that
229 either the channeltron or the ion-collector channel could, independent of each other, start
230 a measurement cycle (EVD = C, I); detection thresholds for ion-collector, channeltron and
231 electron-channel set to the lowest levels and the detection threshold for the entrance grid
232 set to the first digital step (SSEN = 0, 0, 0, 1). See Paper I for a description of these terms.

233 During the entire Ulysses mission dedicated noise tests were performed at monthly in-
234 tervals in order to monitor instrument health and noise characteristics. During all these
235 tests the operational settings were changed in four steps at one-hour intervals, starting
236 from the nominal configuration described above: a) set the event definition status such
237 that the channeltron, the ion collector and the electron-channel can initiate a measure-
238 ment cycle (EVD = C, I, E); b) set the thresholds for all channels to their lowest lev-
239 els (SSEN = 0, 0, 0, 0); c) reset the event definition status to its nominal configuration
240 (EVD = C, I) and increase the channeltron high voltage by one step with respect to the
241 nominal configuration; d) reset the instrument to its nominal configuration (i.e. reduce the
242 channeltron high voltage by one step and set the detection thresholds to SSEN = 0, 0, 0, 1).

243 The noise tests performed in the earlier mission before 2000 revealed a long-term drop
244 in the noise sensitivity of the instrument which was most likely caused by a reduction in
245 the channeltron amplification due to electronics degradation (Paper IX and Krüger et al.,
246 2005b). To counterbalance the reduced amplification we increased the channeltron high
247 voltage by one digital step in August 2000 (HV = 4, 1250 V) which raised the instrument
248 sensitivity close to its original value from the earlier mission again (Paper IX). Although
249 the aging of the channeltron led to a drop in the number of class 3 impacts, the dust impacts
250 which have caused these events should have shown up in lower quality classes. The noise
251 response of the Ulysses dust detector was monitored since then and no significant drop
252 in the sensitivity was recognized. In the time interval considered here HV=4, EVD=C,I,
253 SSEN=0001 was the nominal configuration of the dust instrument (during noise tests the
254 channeltron voltage was always raised by one digital step, i.e. to HV = 5, 1370 V).

255 Figure 3 shows the noise rate of the dust instrument for the 2005 to 2007 period. The upper
256 panel shows the daily maxima of the noise rate. In the earlier mission before November
257 2001 the daily maxima were dominated by noise due to interference with the sounder of

258 the Unified RADio and Plasma wave instrument (URAP) on board Ulysses (Stone et al.,
259 1992). Since November 2001 the sounder was switched off permanently for power saving
260 and no sounder noise occurred anymore (see Papers III, V, VII and IX for details of the
261 sounder operation and sounder-related noise). Individual sharp spikes in the upper panel
262 of Figure 3 are caused by noise tests which occurred at approximately monthly intervals,
263 They are best seen in 2007 when Ulysses was close to the Sun which is known to be a
264 strong source of noise.

265 The bottom panel of Figure 3 shows the daily averages in the noise rate. The average
266 was about 10 events per day at random times and it shows that dead time is negligible.
267 These noise rates are very similar to those measured since August 2000 (Paper IX) when
268 the instrument was operated with the same channeltron voltage as in the 2005-07 interval,
269 implying that no significant channeltron degradation has occurred since 2000.

270 **3 Impact events**

271 The dust instrument classifies all impact events into four classes and six ion charge ampli-
272 tude ranges which leads to 24 individual categories, with one accumulator belonging to one
273 individual category. Class 3, our highest class, are real dust impacts and class 0 are mostly
274 noise events. Depending upon the noise of the charge measurements, classes 1 and 2 can be
275 true dust impacts or noise events. Two classification schemes were used in the Ulysses dust
276 instrument: since 26 March 2002, when the dust instrument was reprogrammed, the clas-
277 sification scheme has been the same as the one used in the Galileo instrument (described
278 in Paper IV). A different scheme was used before which is described in Paper I.

279 Between 1 January 2005 and 30 November 2007 the complete data sets (sensor orientation,
280 charge amplitudes, charge rise times, etc.) of 6970 events including 609 dust impacts were
281 transmitted to Earth. Table 3 lists the number of all dust impacts counted with the 24
282 accumulators of the instrument. ‘AC xy ’ refers to class number ‘ x ’ and amplitude range
283 ‘ y ’ (for a detailed description of the accumulator categories see Paper I). As discussed in
284 the previous section, most noise events were recorded during the time periods when the
285 dust instrument was configured to its high sensitive state for noise tests. During these
286 periods many events were only counted by one of the 24 accumulators because their full
287 information was overwritten before the data could be transmitted to Earth. Since the dust
288 impact rate was low during times outside these periods, it is expected that only the data
289 sets of very few true dust impacts were lost.

290 Table 4 lists all 609 particles detected between January 2005 and November 2007 for which
291 the complete information exists. Note that approximately 45 jovian stream particles were
292 detected in six dust streams in 2005 (AR1, Krüger et al., 2006c) which are about 10 nm
293 in size and their velocities exceed 200km s^{-1} (Zook et al., 1996). Their mass and speed
294 calibration is unreliable because their masses and speeds are outside of the calibration
295 range of the dust instrument.

296 In Table 4 dust particles are identified by their sequence number and their impact time.

297 The event category – class (CLN) and amplitude range (AR) – are given. Raw data as
298 transmitted to Earth are displayed in the next columns: sector value (SEC) which is the
299 spacecraft spin orientation at the time of impact, impact charge numbers (IA, EA, CA) and
300 rise times (IT, ET), time difference and coincidence of electron and ion signals (EIT, EIC),
301 coincidence of ion and channeltron signal (IIC), charge reading at the entrance grid (PA)
302 and time (PET) between this signal and the impact. Then the instrument configuration
303 is given: event definition (EVD), charge sensing thresholds (ICP, ECP, CCP, PCP) and
304 channeltron high voltage step (HV). See Paper I for further explanation of the instrument
305 parameters.

306 The next four columns in Table 4 give information about Ulysses’ orbit: heliocentric dis-
307 tance (R), ecliptic longitude and latitude (LON, LAT) and distance from Jupiter (D_{Jup} , in
308 astronomical units). The next column gives the rotation angle (ROT) as described in Sec-
309 tion 2. Then follows the pointing direction of the dust instrument at the time of particle
310 impact in ecliptic longitude and latitude (S_{LON} , S_{LAT}). Mean impact velocity (v , in km s^{-1})
311 and velocity error factor (VEF, i.e. multiply or divide stated velocity by VEF to obtain
312 upper or lower limits) as well as mean particle mass (m , in grams) and mass error factor
313 (MEF) are given in the last columns. For $\text{VEF} > 6$, both velocity and mass values should
314 be discarded. This occurs for 72 impacts. No intrinsic dust charge values are given (see
315 Svestka et al., 1996, for a detailed analysis). Recently, reliable charge measurements for
316 interplanetary dust grains were reported for the Cassini dust detector (Kempf et al., 2004).
317 These measurements may lead to an improved understanding of the charge measurements
318 of Ulysses and Galileo in the future.

319 4 Analysis

320 The most important impact parameter determined by the dust instrument is the positive
321 charge measured on the ion collector, Q_{I} , because it is relatively insensitive to noise. Fig-
322 ure 4 shows the distribution of Q_{I} for all dust particles detected from 2005 to 2007. Ion
323 impact charges have been detected over the entire range of six orders of magnitude in im-
324 pact charge that the dust instrument can measure. One impact is close to the saturation
325 limit of $\sim 10^{-8} \text{ C}$ and may thus constitute a lower limit of the actual impact charge. The
326 impact charge distribution of the big particles ($Q_{\text{I}} > 10^{-13} \text{ C}$) follows a power law distri-
327 bution with index -0.45 and is shown as a dashed line. This value is very similar to earlier
328 Ulysses measurements of 2000 to 2004 (-0.40 ; cf. Paper IX).

329 In the earlier 1993 to 2004 data set (Papers V, VII and IX) the impact charge distribution
330 was reminiscent of three individual populations: small particles with impact charges $Q_{\text{I}} <$
331 10^{-13} C (AR1), intermediate size particles with $10^{-13} \text{ C} \leq Q_{\text{I}} \leq 10^{-11} \text{ C}$ (AR2 and AR3)
332 and big particles with $Q_{\text{I}} > 10^{-11} \text{ C}$ (AR4 to AR6). This is also visible in the present
333 data set, although less pronounced. The intermediate particles are mostly of interstellar
334 origin and the big particles are attributed to interplanetary grains (Grün et al., 1997, see
335 also Section 5). The small particle impacts (AR1) detected over the polar regions of the

336 Sun are candidates for being interplanetary β -meteoroids (Hamilton et al., 1996; Wehry
337 and Mann, 1999; Wehry et al., 2004).

338 It should be noted that the charge distribution shown in Figure 4 is very similar to the
339 one measured with Galileo in interplanetary space between 1993 and 1995 (i.e. between
340 1 and 5 AU; Paper IV). In particular, the power law index of -0.43 for the big particles
341 was practically identical. This indicates that both dust instruments basically detected the
342 same dust populations in interplanetary space and that their responses to dust impacts are
343 very similar. The only significant difference is a dip in the Ulysses charge distribution at
344 $2 \cdot 10^{-10} \text{ C}$ (Figure 4) which is also evident in all earlier Ulysses data (Papers III, V, VII
345 and IX). In particular, it is visible in both the ecliptic and out-of-ecliptic phases of Ulysses
346 which indicates that it is not sensitive to the impact speed or the dust population of the
347 grains. A small but much weaker dip is also seen in some but not all Galileo data sets. We
348 therefore conclude that the dip is most likely due to an artefact in the Ulysses instrument
349 electronics in AR5.

350 The ratio of the channeltron charge Q_C and the ion collector charge Q_I is a measure of
351 the channeltron amplification A , which in turn is an important parameter for dust impact
352 identification (Paper I). In Figure 5 we show the charge ratio Q_C/Q_I as a function of Q_I for
353 the 2005 to 2007 dust impacts with the channeltron high voltage set to 1250 V ($HV = 4$).
354 This diagram is directly comparable with similar diagrams in the previous Papers III, V
355 and VII for $HV = 3$ and Paper IX for $HV = 4$, respectively.

356 The mean amplification determined from particles with $10^{-12} \text{ C} \leq Q_I \leq 10^{-11} \text{ C}$ and $HV = 4$
357 in the 2005 to 2007 interval is $A \simeq 1.57$. This value is somewhat lower than the values
358 derived from the first five years of the mission (1990 to 1995; Papers III and V) and com-
359 parable to the more recent determinations (1996 to 2004; Papers VII and IX). It indicates
360 that a sufficiently high channeltron amplification and stable instrument operation could be
361 maintained with this higher voltage ($HV = 4$) since 2000. It shows in particular that the
362 channeltron degradation could be mostly counterbalanced by increasing the high voltage
363 by one digital step. Much more severe electronics degradation was found for the Galileo
364 dust detector during Galileo's orbital tour in the jovian system. It was likely related to
365 the harsh radiation environment in the magnetosphere of the giant planet (Krüger et al.,
366 2005b).

367 In Figure 6 we show the masses and velocities of all dust particles detected between 2005
368 and 2007. As in the earlier periods before 2005, velocities occur over the entire calibrated
369 range from 2 to 70 km s^{-1} . The masses vary over almost nine orders of magnitude from
370 $\sim 10^{-7} \text{ g}$ to 10^{-16} g . The mean errors are a factor of 2 for the velocity and a factor of
371 10 for the mass. The clustering of the velocity values is due to discrete steps in the rise
372 time measurement but this quantisation is much smaller than the velocity uncertainty. For
373 many particles in the lowest two amplitude ranges (AR1 and AR2) the velocity had to be
374 computed from the ion charge signal alone which leads to the vertical striping in the lower
375 mass range in Figure 6 (most prominent above 10 km s^{-1}). In the higher amplitude ranges
376 the velocity could normally be calculated from both the target and the ion charge signal,
377 resulting in a more continuous distribution in the mass-velocity plane. Impact velocities

378 below about 3 km s^{-1} should be treated with caution because anomalous impacts onto the
379 sensor grids or structures other than the target generally lead to prolonged rise times and
380 hence to unnaturally low impact velocities.

381 **5 Discussion**

382 In Figure 7 we show the dust impact rate detected in various amplitude ranges together
383 with the total impact rate summed over all amplitude ranges. The highest overall impact
384 rate was recorded in 2007 when Ulysses was in the inner solar system and relatively close
385 to the ecliptic plane. It coincides with a peak in the rate of bigger particles in the three
386 highest ion amplitude ranges (AR4 – AR6). These impacts are attributed to interplanetary
387 particles on low inclination orbits (Grün et al., 1997). The majority of them are the impacts
388 with $Q_I > 10^{-10} \text{ C}$ shown in Figure 4. The impact rate of intermediate sized particles in
389 AR2 and AR3 showed relatively little variation. This size range is dominated by interstellar
390 impactors. The details of the various dust populations are discussed further below.

391 Figure 8 shows the sensor orientation at the time of a particle impact (rotation angle). The
392 big particles (diamonds, impact charge $Q_I \geq 8 \cdot 10^{-14} \text{ C}$ which roughly corresponds to
393 AR2-6) are concentrated towards the upstream direction of interstellar helium (cf. Fig-
394 ure 10, bottom panel; Witte et al., 1996; Witte, 2004; Witte et al., 2004). They have been
395 detected with a relatively constant rate during the entire three-year period (Figure 7). The
396 particles with the highest ion amplitude ranges (AR4 to AR6) are not distinguished in this
397 diagram because they cannot be separated from interstellar particles by directional argu-
398 ments alone. They have to be distinguished by other means (e. g. mass and speed). In
399 addition, their total number is so small that they constitute only a small ”contamination“ of
400 the interstellar particles in Figure 8. In the ecliptic plane at 1.3 AU, however, interplanetary
401 particle flux dominates over interstellar flux by a factor of about 3 (in number).

402 **5.1 Interstellar dust**

403 Interstellar particles move on hyperbolic trajectories through the solar system and approach
404 Ulysses from the same direction as the interstellar gas (Grün et al., 1994; Baguhl et al.,
405 1995a; Witte et al., 1996; Witte, 2004; Witte et al., 2004). They can therefore be identified
406 by their impact direction and their impact speed. Earlier investigations showed that in the
407 Ulysses and Galileo dust data sets the interstellar impactors are mostly found in amplitude
408 ranges AR2 and AR3.

409 In the earlier mission from 1993 to 2004 the impact rate of interstellar grains (as derived
410 from the AR2 and AR3 accumulators) varied by about a factor of 2.5: between 1993 and
411 1995 the rate was $\sim 2 \cdot 10^{-6} \text{ s}^{-1}$ (Paper V) while in the 1996 to 1999 interval it dropped
412 to $\sim 8 \cdot 10^{-7} \text{ s}^{-1}$ (Paper VII) and from 2000 to 2004 the average impact rate was again
413 $\sim 2 \cdot 10^{-6} \text{ s}^{-1}$ (Paper IX). In 2005/2006 the average impact rate of interstellar impactors
414 was somewhat higher: $\sim 3 \cdot 10^{-6} \text{ s}^{-1}$ (bottom panel of Figure 7). In 2007, when Ulysses

415 was in the inner solar system again, the impact rate derived from AR2 and AR3 was still
416 higher. Here, however, the impact rate is not due to interstellar particles alone because of a
417 strong contribution from interplanetary impactors.

418 The dashed curve in Figure 7 (bottom panel) shows the expected impact rate of interstel-
419 lar particles assuming that they approach from the direction of interstellar helium (Witte
420 et al., 1996; Witte, 2004; Witte et al., 2004) and that they move through the solar system
421 on straight trajectories with a relative velocity of 26 km s^{-1} . This assumption means dy-
422 namically that radiation pressure cancels gravity for these particles ($\beta = 1$) and that their
423 Larmor radii are large compared with the dimension of the solar system. Both assumptions
424 are reasonable for particles with masses between 10^{-13} and 10^{-12} g which is the dominant
425 size range measured for interstellar grains (Grün et al., 1997). The variation predicted by
426 the model is caused by changes in the instrument’s viewing direction with respect to the
427 approach direction of the particles and changes in the relative velocity between the space-
428 craft and the particles. The dust particle flux is independent of heliocentric distance in this
429 simple model, which gives relatively good agreement with the observed impact rate.

430 Ulysses has monitored the interstellar dust flow through the solar system for more than 15
431 years. This time period covers more than two and a half revolutions of the spacecraft about
432 the Sun through more than 2/3 of a complete 22-year solar cycle. Thus, Ulysses measured
433 interstellar dust during solar minimum and solar maximum conditions of the interplanetary
434 magnetic field (IMF). The interstellar dust flux modulation due to grain interaction with
435 the magnetic field during solar minimum could be well explained (Landgraf, 1998, 2000;
436 Landgraf et al., 2003). By taking into account the sensor side wall in the instrument field
437 of view we could recently improve the flux determination (Altobelli et al., 2004).

438 Ulysses provides the unique opportunity to compare repeated dust measurements at the
439 same locations in the solar system for different phases of the solar cycle and the inter-
440 planetary magnetic field. In Figure 9 we show the approach direction of interstellar grains
441 for three selected periods when Ulysses was between approximately -8 and -56° ecliptic
442 latitude during approach to the inner solar system. During these three intervals the dust de-
443 tection geometry as indicated by the contour lines was very similar so that we can compare
444 them directly. At least three differences are obvious between the three panels:

- 445 • The approach direction of the majority of grains was compatible with the flow di-
446 rection of the interstellar helium gas as measured with Ulysses (Witte, 2004; Witte
447 et al., 2004) during all three time intervals.
- 448 • The dust flux varied by a factor of about two during the three intervals, the lowest
449 flux being measured in the period 1999 to 2000, while the highest flux occurred in
450 2005/2006 (Krüger et al., 2007).
- 451 • A subset of the grains detected in 2005 shows a clear shift in the detected impact
452 direction away from the ecliptic plane towards southern ecliptic latitudes.

453 Our preliminary analysis indicates that this shift is about 30° away from the ecliptic plane
454 towards southern ecliptic latitudes (Krüger et al., 2007). The reason for this shift remains

455 mysterious. Whether it is connected to a secondary stream of interstellar neutral atoms
456 shifted from the main neutral gas flow (Collier et al., 2004; Wurz et al., 2004; Nakagawa
457 et al., 2006) is presently unclear. Given, however, that the neutral gas stream is shifted
458 along the ecliptic plane while the shift in the dust flow is offset from the ecliptic, a connec-
459 tion between both phenomena seems unlikely.

460 Even though Ulysses' position in the heliosphere and the dust detection conditions were
461 very similar during all three time intervals considered in Figure 9, the configurations of the
462 solar wind driven interplanetary magnetic field (IMF), which strongly affects the dynamics
463 of the smallest grains, were completely different. We have to consider that the interstellar
464 grains need approximately twenty years to travel from the heliospheric boundary to the
465 inner solar system where they are detected by Ulysses. Thus, the effect of the IMF on
466 the grain dynamics is the accumulated effect caused by the interaction with the IMF over
467 several years: In the earlier time intervals (1993/1994 and 1999/2000) the grains had a
468 recent dynamic history dominated by solar minimum conditions (Landgraf, 2000), while
469 the grains detected during the third interval (2005/2006) had a recent history dominated by
470 the much more disturbed solar maximum conditions of the IMF. During the solar maximum
471 conditions the overall magnetic dipole field changed polarity. Morfill and Grün (1979)
472 predicted that due to this effect in a 22-year cycle, small interstellar grains experience either
473 focussing or defocusing conditions. During these times they are systematically deflected
474 by the solar wind magnetic field either towards or away from the solar magnetic equator
475 plane (close to the ecliptic plane). This latter configuration likely has a strong influence on
476 the dust dynamics and the total interstellar flux in the inner heliosphere but it has not been
477 modelled in detail. An explanation of the grain interaction with the IMF at the recent solar
478 maximum conditions is still pending.

479 Detailed modelling of the dynamics of the electrically charged dust grains in the helio-
480 sphere can give us information about the local interstellar environment of the solar system
481 where the particles originate from. The models developed by Landgraf et al. (2003) fit the
482 observed flux variation by assuming a constant dust concentration in the local interstellar
483 environment of our solar system. It implies that the local interstellar dust phase must be
484 homogeneously distributed over length scales of 50 AU, which is the distance travelled by
485 the Sun during the measurement period of Ulysses from 1992 to 2002. This conclusion
486 is supported by the more recent Ulysses data until the end of 2004 (Krüger et al., 2006a).
487 Our latest Ulysses dust data of 2005/2006, on the other hand, put a question mark onto
488 this conclusion because if the observed shift in impact direction turns out to be intrinsic, it
489 would imply that this homogeneity breaks down on larger length scales.

490 **5.2 Interplanetary dust**

491 Figure 10 shows the data (AR3 to AR6) from launch in 1990 until the end of the Ulysses
492 mission in 2007 and compares them with two meteoroid environment models by Divine
493 (1993) and Staubach et al. (1997). For most of the mission time, excluding the ecliptic
494 plane crossings in 1995, 2001 and 2007 the Divine model predicts impacts from a very

495 broad range of directions, with spin angles from 45° to 300° . The impactors belong mostly
496 to the so-called "halo" population which was introduced in the model to explain the Pioneer
497 data (Divine, 1993). The Ulysses directionality of the impacts had not been available at the
498 time of construction of the model, and they are not well fit by the "halo" population. In
499 contrast, the Staubach et al. (1997) model was fit to 5 years of Ulysses data from the craft's
500 first orbit about the Sun, taking the crucial directional information into account. It is in
501 better agreement with the data and has been confirmed by Ulysses' second and third orbits.
502 It places most of the impacts into the spin angle range from 30° to 120° . These are due to
503 interstellar dust flowing through the solar system (Grün et al., 1994).

504 One more observation from these plots is that both the Divine and Staubach models predict
505 higher flux during the ecliptic plane crossings than the data permit. The time dependence
506 of the interstellar dust flux was asserted after the meteoroid models under review had been
507 constructed (Landgraf, 2000). However, the disagreement at the ecliptic plane crossings
508 was not anticipated, since almost all data incorporated in the models were taken from the
509 ecliptic plane. Possible explanations of the discrepancy are the roughness of model fits as
510 well as different representations of the data taken for model adjustments and displayed in
511 Figure 10. While Figure 10 selects all impacts above a fixed threshold of charge released,
512 the models were fitted using more uncertain inferred mass thresholds. The inference of
513 mass is based on speed determination that is uncertain by a factor of 2.

514 **5.3 β -meteoroids**

515 When Ulysses was in the inner solar system in 1995 and in 2001, maxima were evident in
516 the impact rate of the smallest particles (AR1; Papers V and IX). A similar maximum in the
517 inner solar system occurred again in 2007 (Fig. 7; top panel). Although in all three cases the
518 maximum was reached during a short period around ecliptic plane crossing, many particles
519 were also detected at high ecliptic latitudes. These grains are attributed to a population of
520 submicron-sized interplanetary particles whose dynamics is dominated by solar radiation
521 pressure. They move on escape trajectories from the solar system (β -meteoroids, Baguhl
522 et al., 1995b; Hamilton et al., 1996). β -meteoroids were identified with Ulysses over the
523 Sun's poles in 1994/95 (Wehry and Mann, 1999) and 2000/01 (Wehry et al., 2004). Due
524 to the detection geometry, however, they were undetectable outside these periods, explain-
525 ing the lower impact rates in AR1. β -meteoroids were detectable again from mid-2006
526 until early-2008 (Wehry et al., 2004). In independent potential detection of β -meteoroids
527 was recently reported from the plasma wave instrument on board the STEREO spacecraft
528 (Meyer-Vernet et al., 2009).

529 Wehry and Mann (1999) and Wehry et al. (2004) identified a significant asymmetry in the
530 flux of these particles between the northern and the southern hemisphere from the first two
531 heliocentric orbits of Ulysses, the reason of which is presently unknown. A comprehensive
532 analysis of these three data sets will be the subject of a future investigation and may reveal
533 whether the asymmetry is connected with the solar cycle variation of the interplanetary
534 magnetic field.

535 6 Conclusions

536 In this paper, the eleventh and final in a series of Ulysses and Galileo dust data papers, we
537 present data from the Ulysses dust instrument for the period January 2005 to November
538 2007. In this time interval, starting from a heliocentric distance of 5.3 AU close to aphelion,
539 the spacecraft approached the Sun, flew over the Sun's south pole, crossed the ecliptic plane
540 at 1.4 AU heliocentric distance and reached a northern ecliptic latitude of 60° .

541 A total number of 609 dust impacts were recorded during this period. Together with 6110
542 impacts recorded in interplanetary space and near Jupiter between Ulysses' launch in Oc-
543 tober 1990 and December 2004 (Grün et al., 1995a; Krüger et al., 1999b, 2001b, 2006a),
544 the complete dust data set measured during the entire Ulysses mission consists of 6719
545 impacts. Given its temporal coverage and Ulysses' unique orbital orientation, the Ulysses
546 dust data set will be a treasure for decades to come.

547 The total recorded dust impact rate dropped from an initial value of 0.7 impacts per day in
548 2005 when Ulysses was at low ecliptic latitudes to a value of 0.3 impacts at higher latitudes.
549 Most of these particles were of interstellar origin, in particular at higher ecliptic latitudes,
550 a minor fraction being interplanetary particles. A maximum of 1.5 per day was measured
551 in 2007 in the inner solar system; here the majority of the grains were of interplanetary
552 origin.

553 The measurements from the entire Ulysses mission since launch in 1990 are in disagree-
554 ment with the interplanetary dust flux model by Divine (1993). Instead, they are well
555 matched by the model of Staubach et al. (1997) which was originally developed with a
556 shorter data set from the first Ulysses orbit and with the dust measurements from Galileo's
557 interplanetary cruise.

558 Noise tests performed regularly during the three years period revealed no degradation in
559 the noise sensitivity of the dust instrument, and the nominal instrument operational con-
560 figuration remained unchanged during the entire period. In particular, no change in the
561 channeltron high voltage setting was required.

562 With Ulysses we had the unprecedented opportunity to measure dust in interplanetary space
563 for approximately 17 years. In particular, due to the unique orientation of Ulysses' orbital
564 plane approximately perpendicular to the flow direction of the interstellar dust through the
565 solar system and the spacecraft's 6-year revolution period about the Sun, we obtained dust
566 measurements from three traverses of the same spatial region at southern ecliptic latitudes.
567 These passes were separated by six years in time and were obtained at different phases of
568 the solar cycle. Variations in the interstellar dust flux by a factor of three are evident during
569 the entire mission. Flux variations until 2002 have been explained by the interaction of the
570 dust grains with the time-varying interplanetary magnetic field, while detailed modelling
571 of the later data is still pending. The data obtained in 2005/2006 reveal an approximately
572 30° shift in the approach direction of the grains away from the approach direction of the
573 interstellar helium gas. The reason for this shift remains mysterious and will be the subject
574 of a future investigation.

575 Even though this is the final paper in our series of Ulysses dust data papers published

576 during the last 15 years, the evaluation of this unique data set is continuing. A list of
577 specific open questions raised in this and earlier data papers includes:

- 578 • *β -meteoroids*: The detailed evaluation of the measurements from Ulysses' third so-
579 lar orbit is still pending. Open questions include the measured north-south asym-
580 metry in the measured flux and the heliocentric distance range where these grains
581 are generated. More measurements from other spacecraft (e.g. STEREO) would be
582 advantageous to answer these questions.

- 583 • *Comparison with Pioneer 10 and 11 measurements*: The flux of particles with $m \geq$
584 10^{-9} g as measured with Ulysses is about a factor of five lower than expected from
585 the Pioneer 10/11 measurements. Potential reasons for this discrepancy are errors
586 on the mass calibrations of the Ulysses and/or Pioneer detectors in this mass range,
587 many of the Pioneer detections may not be due to actual meteoroid impacts, or the
588 dust grains by Pioneer belong to a population of dust which could not or only parti-
589 tially be detected with Ulysses (Krüger et al., 1999b). Measurements with New
590 Horizons in the outer solar system may shed new light onto this question.

- 591 • *Interstellar dust*: Earlier comprehensive investigations of the interstellar impactors
592 were mostly performed in the late 1990s and relied upon the significantly smaller
593 data set available at the time. In the meantime, until the end of the Ulysses mission,
594 the interstellar dust data set has grown by at least a factor of two so that a complete
595 re-analysis of the entire data set is worthwhile and can give new insights into, e.g., the
596 grain dynamics inside the heliosphere and into the conditions in the local interstellar
597 environment where these grains originate from. In particular, the reason for the
598 observed 30° shift remains an open question.

- 599 • *Interplanetary dust*: The interplanetary dust model by Divine (1993) was developed
600 before the Ulysses data became available and the model by Staubach et al. (1997)
601 used only data from within the ecliptic plane and from a fraction of Ulysses' first
602 heliocentric orbit. A new model is presently being developed by Dikarev et al. (2005)
603 which will incorporate infrared observations of the zodiacal cloud by the COBE
604 DIRBE instrument, in-situ flux measurements by the dust detectors on board Galileo
605 and Ulysses, and the crater size distributions on lunar rock samples retrieved by the
606 Apollo missions.

607 **Acknowledgements.** We dedicate this work to the memory of Dietmar Linkert who passed
608 away in spring 2009. He was Principal Engineer for space instruments at MPI für Kern-
609 physik including the dust instruments flown on the HEOS-2, Helios, Galileo, Ulysses and
610 Cassini missions. His friends and colleagues around the world appreciated his experience
611 and sought his professional advice. We thank the Ulysses project at ESA and NASA/JPL
612 for effective and successful mission operations. This work has been supported by the
613 Deutsches Zentrum für Luft- und Raumfahrt e.V. (DLR) under grants 50 0N 9107 and
614 50 QJ 9503. Support by Max-Planck-Institut für Kernphysik and Max-Planck-Institut für
615 Sonnensystemforschung is also gratefully acknowledged.

616 References

- 617 Altobelli, N., Kempf, S., Krüger, H., Landgraf, M., Srama, R., and Grün, E.: 2005a, *In-Situ*
618 *Monitoring of Interstellar Dust in the Inner Solar System*, in *AIP Conf. Proc. 761: The*
619 *Spectral Energy Distributions of Gas-Rich Galaxies: Confronting Models with Data*, pp
620 149–152
- 621 Altobelli, N., Kempf, S., Krüger, H., Landgraf, M., Roy, M., and Grün, E.: 2005b, *Inter-*
622 *stellar dust flux measurements by the Galileo dust instrument between Venus and Mars*
623 *orbit, Journal of Geophysical Research* **110**, 7102–7115
- 624 Altobelli, N., Kempf, S., Landgraf, M., Srama, R., Dikarev, V., Krüger, H., Moragas-
625 Klostermeyer, G., and Grün, E.: 2003, *Cassini between Venus and Earth: Detection of*
626 *Interstellar Dust, Journal of Geophysical Research* **108**, A10, 7–1
- 627 Altobelli, N., Moissl, R., Krüger, H., Landgraf, M., and Grün, E.: 2004, *Influence of wall*
628 *impacts on the Ulysses dust detector in modelling the interstellar dust flux, Planetary*
629 *and Space Science* **52**, 1287–1295
- 630 Baggaley, W. J. and Neslušan, L.: 2002, *A model of the heliocentric orbits of a stream of*
631 *Earth-impacting interstellar meteoroids, Astronomy and Astrophysics* **382**, 1118–1124
- 632 Baguhl, M., Grün, E., Hamilton, D. P., Linkert, G., Riemann, R., and Staubach, P.: 1995a,
633 *The flux of interstellar dust observed by Ulysses and Galileo, Space Science Reviews*
634 **72**, 471–476
- 635 Baguhl, M., Hamilton, D. P., Grün, E., Dermott, S. F., Fechtig, H., Hanner, M. S., Kissel,
636 J., Lindblad, B. A., Linkert, D., Linkert, G., Mann, I., McDonnell, J. A. M., Morfill,
637 G. E., Polanskey, C., Riemann, R., Schwehm, G. H., Staubach, P., and Zook, H. A.:
638 1995b, *Dust measurements at high ecliptic latitudes, Science* **268**, 1016–1020
- 639 Balogh, A., Marsden, R., and Smith, E. e.: 2001, *The heliosphere near solar minimum:*
640 *The Ulysses Perspective*, Springer Praxis, Springer, Berlin, Heidelberg, New York
- 641 Collier, M. R., Moore, T. E., Simpson, D., Roberts, A., Szabo, A., Fuselier, S., Wurz, P.,
642 Lee, M. A., and Tsurutani, B. T.: 2004, *An unexplained 10 – 40° shift in the location of*
643 *some diverse neutral atom data at 1 AU, Advances in Space Research* **34**, 166–171
- 644 Czechowski, A. and Mann, I.: 2003a, *Local interstellar cloud grains outside the he-*
645 *liopause, Astronomy and Astrophysics* **410**, 165–173
- 646 Czechowski, A. and Mann, I.: 2003b, *Penetration of Interstellar Grains into the Helio-*
647 *sphere, Journal of Geophysical Research* **108**, A10, 8038, 10.1029/2003JA009917
- 648 Dikarev, V., Landgraf, M., Grün, E., Baggaley, W., and Galligan, D.: 2001, *Interplanetary*
649 *Dust Model: From Micron sized Dust to Meteors, Proceedings of the Meteoroids 2001*
650 *Conference* pp 609–615

- 651 Dikarev, V., Jehn, R., and Grün, E.: 2002, *Towards a new model of the interplanetary*
652 *meteoroid environment*, *Advances in Space Research* **29(8)**, 1171–1175
- 653 Dikarev, V., Grün, E., Baggaley, J., Galligan, D., Landgraf, M., and Jehn, R.: 2005, *The*
654 *new ESA meteoroid model*, *Advances in Space Research* **35**, 1282–1289
- 655 Divine, N.: 1993, *Five populations of interplanetary meteoroids*, *Journal of Geophysical*
656 *Research* **98**, 17029–17048
- 657 Flandes, A. and Krüger, H.: 2007, *Solar wind modulation of Jupiter dust stream detection*,
658 in H. Krüger and A. L. Graps (ed.), *Dust in planetary systems*, pp 87–90, ESA SP-643
- 659 Flandes, A., Krüger, H., Hamilton, D. P., and Valdés-Galicia, J. F.: 2009, *Magnetic field*
660 *modulated dust streams from Jupiter in interplanetary space*, *Icarus*, in preparation
- 661 Frisch, P. C., Dorschner, J., Geiß, J., Greenberg, J. M., Grün, E., Landgraf, M., Hoppe,
662 P., Jones, A. P., Krätschmer, W., Linde, T. J., Morfill, G. E., Reach, W. T., Slavin,
663 J., Svestka, J., Witt, A., and Zank, G. P.: 1999, *Dust in the Local Interstellar Wind*,
664 *Astrophysical Journal* **525**, 492–516
- 665 Frisch, P. C. and Slavin, J. D.: 2003, *The Chemical Composition and Gas-to-Dust Mass*
666 *Ratio of Nearby Interstellar Matter*, *Astrophysical Journal* **594**, 844–858
- 667 Graps, A. L., Grün, E., Svedhem, H., Krüger, H., Horányi, M., Heck, A., and Lammers,
668 S.: 2000, *Io as a source of the Jovian dust streams*, *Nature* **405**, 48–50
- 669 Grün, E., Fechtig, H., Hanner, M. S., Kissel, J., Lindblad, B. A., Linkert, D., Maas, D.,
670 Morfill, G. E., and Zook, H. A.: 1992a, *The Galileo dust detector*, *Space Science*
671 *Reviews* **60**, 317–340
- 672 Grün, E., Fechtig, H., Kissel, J., Linkert, D., Maas, D., McDonnell, J. A. M., Morfill, G. E.,
673 Schwehm, G. H., Zook, H. A., and Giese, R. H.: 1992b, *The Ulysses dust experiment*,
674 *Astronomy and Astrophysics, Supplement* **92**, 411–423
- 675 Grün, E., Zook, H. A., Baguhl, M., Balogh, A., Bame, S. J., Fechtig, H., Forsyth, R.,
676 Hanner, M. S., Horányi, M., Kissel, J., Lindblad, B. A., Linkert, D., Linkert, G., Mann,
677 I., McDonnell, J. A. M., Morfill, G. E., Phillips, J. L., Polanskey, C., Schwehm, G. H.,
678 Siddique, N., Staubach, P., Svestka, J., and Taylor, A.: 1993, *Discovery of Jovian dust*
679 *streams and interstellar grains by the Ulysses spacecraft*, *Nature* **362**, 428–430
- 680 Grün, E., Gustafson, B. E., Mann, I., Baguhl, M., Morfill, G. E., Staubach, P., Taylor, A.,
681 and Zook, H. A.: 1994, *Interstellar dust in the heliosphere*, *Astronomy and Astrophysics*
682 **286**, 915–924
- 683 Grün, E., Baguhl, M., Divine, N., Fechtig, H., Hamilton, D. P., Hanner, M. S., Kissel,
684 J., Lindblad, B. A., Linkert, D., Linkert, G., Mann, I., McDonnell, J. A. M., Morfill,
685 G. E., Polanskey, C., Riemann, R., Schwehm, G. H., Siddique, N., Staubach, P., and

- 686 Zook, H. A.: 1995a, *Two years of Ulysses dust data*, *Planetary and Space Science* **43**,
687 971–999, Paper III
- 688 Grün, E., Baguhl, M., Divine, N., Fechtig, H., Hamilton, D. P., Hanner, M. S., Kissel,
689 J., Lindblad, B. A., Linkert, D., Linkert, G., Mann, I., McDonnell, J. A. M., Morfill,
690 G. E., Polanskey, C., Riemann, R., Schwehm, G. H., Siddique, N., Staubach, P., and
691 Zook, H. A.: 1995b, *Three years of Galileo dust data*, *Planetary and Space Science* **43**,
692 953–969, Paper II
- 693 Grün, E., Baguhl, M., Hamilton, D. P., Kissel, J., Linkert, D., Linkert, G., and Riemann,
694 R.: 1995c, *Reduction of Galileo and Ulysses dust data*, *Planetary and Space Science*
695 **43**, 941–951, Paper I
- 696 Grün, E., Staubach, P., Baguhl, M., Hamilton, D. P., Zook, H. A., Dermott, S. F., Gustafson,
697 B. A., Fechtig, H., Kissel, J., Linkert, D., Linkert, G., Srama, R., Hanner, M. S.,
698 Polanskey, C., Horányi, M., Lindblad, B. A., Mann, I., McDonnell, J. A. M., Mor-
699 fill, G. E., and Schwehm, G. H.: 1997, *South-North and Radial Traverses through the*
700 *Interplanetary Dust Cloud*, *Icarus* **129**, 270–288
- 701 Grün, E., Krüger, H., Graps, A., Hamilton, D. P., Heck, A., Linkert, G., Zook, H., Dermott,
702 S. F., Fechtig, H., Gustafson, B., Hanner, M., Horányi, M., Kissel, J., Lindblad, B.,
703 Linkert, G., Mann, I., McDonnell, J. A. M., Morfill, G. E., Polanskey, C., Schwehm,
704 G. H., and Srama, R.: 1998, *Galileo observes electromagnetically coupled dust in the*
705 *Jovian magnetosphere*, *Journal of Geophysical Research* **103**, 20011–20022
- 706 Grün, E. and Landgraf, M.: 2000, *Collisional consequences of big interstellar grains*,
707 *Journal of Geophysical Research* **105 no A5**, 10,291–10,298
- 708 Grün, E., Krüger, H., and Landgraf, M.: 2001, *Cosmic Dust*, in A. Balogh, R. Marsden,
709 and E. Smith (eds.), *The heliosphere at solar minimum: The Ulysses perspective*, pp
710 373–404, Springer Praxis
- 711 Hamilton, D. P. and Burns, J. A.: 1993, *Ejection of dust from Jupiter’s gossamer ring*,
712 *Nature* **364**, 695–699
- 713 Hamilton, D. P., Grün, E., and Baguhl, M.: 1996, *Electromagnetic escape of dust from the*
714 *solar system*, in B. A. S. Gustafson and M. S. Hanner (eds.), *Physics, Chemistry and*
715 *Dynamics of Interplanetary Dust*, *ASP Conference Series*, Vol. 104, pp 31–34
- 716 Horányi, M., Morfill, G. E., and Grün, E.: 1993, *Mechanism for the acceleration and*
717 *ejection of dust grains from Jupiter’s magnetosphere*, *Nature* **363**, 144–146
- 718 Horányi, M., Grün, E., and Heck, A.: 1997, *Modeling the Galileo dust measurements at*
719 *Jupiter*, *Geophysical Research Letters* **24**, 2175–2178
- 720 Jones, G. H. and Balogh, A.: 2003, *A survey of strong interplanetary field enhancements at*
721 *Ulysses*, *Icarus* **166**, 297–310

- 722 Kempf, S., Srama, R., Altobelli, N., Auer, S., Tschernjawski, V., Bradley, J., Burton,
723 M. E., Helfert, S., Johnson, T. V., Krüger, H., Moragas-Klostermeyer, G., and Grün, E.:
724 2004, *Cassini between Earth and asteroid belt: first in-situ charge measurements of*
725 *interplanetary grains*, *Icarus* **171**, 317–335
- 726 Krüger, H., Grün, E., Hamilton, D. P., Baguhl, M., Dermott, S. F., Fechtig, H., Gustafson,
727 B. A., Hanner, M. S., Horányi, M., Kissel, J., Lindblad, B. A., Linkert, D., Linkert, G.,
728 Mann, I., McDonnell, J. A. M., Morfill, G. E., Polanskey, C., Riemann, R., Schwehm,
729 G. H., Srama, R., and Zook, H. A.: 1999a, *Three years of Galileo dust data: II. 1993 to*
730 *1995*, *Planetary and Space Science* **47**, 85–106, Paper IV
- 731 Krüger, H., Grün, E., Landgraf, M., Baguhl, M., Dermott, S. F., Fechtig, H., Gustafson,
732 B. A., Hamilton, D. P., Hanner, M. S., Horányi, M., Kissel, J., Lindblad, B., Linkert,
733 D., Linkert, G., Mann, I., McDonnell, J. A. M., Morfill, G. E., Polanskey, C., Schwehm,
734 G. H., Srama, R., and Zook, H. A.: 1999b, *Three years of Ulysses dust data: 1993 to*
735 *1995*, *Planetary and Space Science* **47**, 363–383, Paper V
- 736 Krüger, H., Grün, E., Graps, A. L., Bindschadler, D. L., Dermott, S. F., Fechtig, H.,
737 Gustafson, B. A., Hamilton, D. P., Hanner, M. S., Horányi, M., Kissel, J., Lindblad,
738 B., Linkert, D., Linkert, G., Mann, I., McDonnell, J. A. M., Morfill, G. E., Polanskey,
739 C., Schwehm, G. H., Srama, R., and Zook, H. A.: 2001a, *One year of Galileo dust data*
740 *from the jovian system: 1996*, *Planetary and Space Science* **49**, 1285–1301, Paper VI
- 741 Krüger, H., Grün, E., Landgraf, M., Dermott, S. F., Fechtig, H., Gustafson, B. A., Hamil-
742 ton, D. P., Hanner, M. S., Horányi, M., Kissel, J., Lindblad, B., Linkert, D., Linkert, G.,
743 Mann, I., McDonnell, J. A. M., Morfill, G. E., Polanskey, C., Schwehm, G. H., Srama,
744 R., and Zook, H. A.: 2001b, *Four years of Ulysses dust data: 1996 to 1999*, *Planetary*
745 *and Space Science* **49**, 1303–1324, Paper VII
- 746 Krüger, H., Forsyth, R. J., Graps, A. L., and Grün, E.: 2005a, *Electromagnetically In-*
747 *teracting Dust Streams During Ulysses' Second Jupiter Encounter*, in Boufendi, L.,
748 Mikikian, M. and Shukla, P. K., AIP conference proceedings (ed.), *New Vistas in Dusty*
749 *Plasmas*, pp 157–160
- 750 Krüger, H., Grün, E., Linkert, D., Linkert, G., and Moissl, R.: 2005b, *Galileo long-term*
751 *dust monitoring in the jovian magnetosphere*, *Planetary and Space Science* **53**, 1109–
752 1120
- 753 Krüger, H., Altobelli, N., Anweiler, B., Dermott, S. F., Dikarev, V., Graps, A. L., Grün,
754 E., Gustafson, B. A., Hamilton, D. P., Hanner, M. S., Horányi, M., Kissel, J., Landgraf,
755 M., Lindblad, B., Linkert, D., Linkert, G., Mann, I., McDonnell, J. A. M., Morfill, G. E.,
756 Polanskey, C., Schwehm, G. H., Srama, R., and Zook, H. A.: 2006a, *Five years of*
757 *Ulysses dust data: 2000 to 2004*, *Planetary and Space Science* **54**, 932–956, Paper IX
- 758 Krüger, H., Bindschadler, D., Dermott, S. F., Graps, A. L., Grün, E., Gustafson, B. A.,
759 Hamilton, D. P., Hanner, M. S., Horányi, M., Kissel, J., Lindblad, B., Linkert, D.,

- 760 Linkert, G., Mann, I., McDonnell, J. A. M., Moissl, R., Morfill, G. E., Polanskey, C.,
761 Schwehm, G. H., Srama, R., and Zook, H. A.: 2006b, *Galileo dust data from the jovian*
762 *system: 1997 to 1999*, *Planetary and Space Science* **54**, 879–910, Paper VIII
- 763 Krüger, H., Graps, A. L., Hamilton, D. P., Flandes, A., Forsyth, R. J., Horányi, M., and
764 Grün, E.: 2006c, *Ulysses jovian latitude scan of high-velocity dust streams originating*
765 *from the jovian system*, *Planetary and Space Science* **54**, 919–931
- 766 Krüger, H., Landgraf, M., Altobelli, N., and Grün, E.: 2007, *Interstellar dust in the solar*
767 *system*, *Space Science Reviews* **130**, 401–408
- 768 Krüger, H. and Grün, E.: 2009, *Interstellar Dust Inside and Outside the Heliosphere*, in
769 Linsky, J. and Izmodenov, V. and Möbius, E. (ed.), *From the outer heliosphere to the*
770 *local bubble*, Springer Heidelberg
- 771 Krüger, H., Bindschadler, D., Dermott, S. F., Graps, A. L., Grün, E., Gustafson, B. A.,
772 Hamilton, D. P., Hanner, M. S., Horányi, M., Kissel, J., Linkert, D., Linkert, G., Mann,
773 I., McDonnell, J. A. M., Moissl, R., Morfill, G. E., Polanskey, C., Roy, M., Schwehm,
774 G. H., and Srama, R.: 2010, *Galileo dust data from the jovian system: 2000 to 2003*,
775 *Planetary and Space Science*, Paper X, submitted
- 776 Landgraf, M.: 1998, *Modellierung der Dynamik und Interpretation der In-situ-Messung in-*
777 *terstellaren Staubs in der lokalen Umgebung des Sonnensystems*, *Ph.D. thesis*, Ruprecht-
778 *Karls-Universität Heidelberg*
- 779 Landgraf, M., Augustsson, K., Grün, E., and Gustafson, B. A. S.: 1999, *Deflection of the*
780 *local interstellar dust flow by solar radiation pressure*, *Science* **286**, 2,319–2,322
- 781 Landgraf, M.: 2000, *Modelling the Motion and Distribution of Interstellar Dust inside the*
782 *Heliosphere*, *Journal of Geophysical Research* **105**, no. **A5**, 10,303–10316
- 783 Landgraf, M., Baggeley, W. J., Grün, E., Krüger, H., and Linkert, G.: 2000, *Aspects*
784 *of the Mass Distribution of Interstellar Dust Grains in the Solar System from in situ*
785 *Measurements*, *Journal of Geophysical Research* **105**, no. **A5**, 10,343–10352
- 786 Landgraf, M., Krüger, H., Altobelli, N., and Grün, E.: 2003, *Penetration of the Heliosphere*
787 *by the interstellar dust stream during solar maximum*, *Journal of Geophysical Research*
788 **108**, 5–1
- 789 Mann, I., Grün, E., and Wilck, M.: 1996, *The Contribution of Asteroid Dust to the Inter-*
790 *planetary Dust Cloud: The Impact of ULYSSES Results on the Understanding of Dust*
791 *Production in the Asteroid Belt and of the Formation of the IRAS Dust Bands*, *Icarus*
792 **120**, 399–407
- 793 Mann, I. and Kimura, H.: 2000, *Interstellar dust properties dervied from mass density,*
794 *mass distribution, and flux rates in the heliosphere*, *Journal of Geophysical Research*
795 **105 No. A5**, 10,317–10,328

- 796 Mann, I., Kimura, H., Biesecker, D. A., Tsurutani, B. T., Grün, E., McKibben, R. B., Liou,
797 J.-C., MacQueen, R. M., Mukai, T., Guhathakurta, M., and Lamy, P.: 2004, *Dust Near*
798 *The Sun*, *Space Science Reviews* **110**, 269–305
- 799 Mann, I. and Czechowski, A.: 2005, *Dust Destruction and Ion Formation in the Inner*
800 *Solar System*, *Astrophysical Journal, Letters* **621**, L73–L76
- 801 Meyer-Vernet, N., Maksimovic, M., Czechowski, A., Mann, I., Zouganelis, I., Goetz, K.,
802 Kaiser, M. L., St. Cyr, O. C., Bougeret, J.-L., and Bale, S. D.: 2009, *Dust Detection by*
803 *the Wave Instrument on STEREO: Nanoparticles Picked up by the Solar Wind?*, *Solar*
804 *Physics* **256**, 463–474
- 805 Morfill, G. E. and Grün, E.: 1979, *The motion of charged dust particles in interplanetary*
806 *space II -Interstellar grains*, *Planetary and Space Science* **27**, 1283–1292
- 807 Nakagawa, H., Bzowski, M., Yamazaki, A., Fukunishi, H., Watanabe, S., Takahashi, Y.,
808 and Taguchi, M.: 2006, *Secondary population of interstellar neutrals seems deflected to*
809 *the side*, in *36th COSPAR Scientific Assembly*, Vol. 36 of *COSPAR, Plenary Meeting*, p
810 1170
- 811 Staubach, P., Grün, E., and Jehn, R.: 1997, *The meteoroid environment near earth*, *Ad-*
812 *vances in Space Research* **19**, 301–308
- 813 Stone, R. G., Bougeret, J. L., Caldwell, J., Canu, P., de Conchy, Y., Cornilleau-Wehrin,
814 N., Desch, M. D., Fainberg, J., Goetz, K., Goldstein, M. L., Harvey, C. C., Hoang, S.,
815 Howard, R., Kaiser, M. L., Kellogg, P., Klein, B., Knoll, R., Lecacheux, A., Langyel-
816 Frey, D., MacDowall, R. J., Manning, R., Meetre, C. A., Meyer, A., Monge, N., Monson,
817 S., Nicol, G., Reiner, M. J., Steinbert, J. L., Torres, E., de Villedary, C., Wouters, F., and
818 Zarka, P.: 1992, *The unified radio and plasma wave investigation*, *Astronomy and*
819 *Astrophysics, Supplement* **92**, 291–316
- 820 Svestka, J., Auer, S., Baguhl, M., and Grün, E.: 1996, *Measurements of dust electric*
821 *charges by the Ulysses and Galileo dust detectors*, in B. A. Gustafson and M. S. Hanner
822 (eds.), *Physics, Chemistry and Dynamics of Interplanetary Dust*, *ASP Conference Series*,
823 Vol. 104, pp 481–484
- 824 Taylor, A. D., Baggeley, W. J., and Steel, D. I.: 1996, *Discovery of interstellar dust*
825 *entering the Earth's atmosphere*, *Nature* **380**, 323–325
- 826 Wehry, A. and Mann, I.: 1999, *Identification of β -meteoroids from measurements of the*
827 *dust detector onboard the Ulysses spacecraft*, *Astronomy and Astrophysics* **341**, 296–
828 303
- 829 Wehry, A., Krüger, H., and Grün, E.: 2004, *Analysis of Ulysses data: Radiation pressure*
830 *effects on dust particles*, *Astronomy and Astrophysics* **419**, 1169–1174

- 831 Wenzel, K., Marsden, R., Page, D., and Smith, E.: 1992, *The Ulysses mission*, *Astronomy*
832 *and Astrophysics, Supplement* **92**, 207–219
- 833 Willis, M. J., Burchell, M., Ahrens, T. J., Krüger, H., and Grün, E.: 2005, *Decreased values*
834 *of cosmic dust number density estimates in the solar system*, *Icarus* **176**, 440–452
- 835 Witte, M., Banaszekiewicz, H., and Rosenbauer, H.: 1996, *Recent results on the parameters*
836 *of interstellar helium from the Ulysses/GAS experiment*, *Space Science Reviews* **78**, no.
837 **1/2**, 289–296
- 838 Witte, M.: 2004, *Kinetic parameters of interstellar neutral helium. Review of results ob-*
839 *tained during one solar cycle with the Ulysses/GAS-instrument*, *Astronomy and Astro-*
840 *physics* **426**, 835–844
- 841 Witte, M., Banaszekiewicz, M., Rosenbauer, H., and McMullin, D.: 2004, *Kinetic param-*
842 *eters of interstellar neutral helium: updated results from the Ulysses/GAS instrument*,
843 *Advances in Space Research* **34**, 61–65
- 844 Wurz, P., Collier, M. R., Moore, T. E., Simpson, D., Fuselier, S., and Lennartson, W.: 2004,
845 *Possible Origin of the Secondary Stream of Neutral Fluxes at 1 AU*, in V. Florinski, N. V.
846 Pogorelov, and G. P. Zank (eds.), *Physics of the Outer Heliosphere*, Vol. 719 of *American*
847 *Institute of Physics Conference Series*, pp 195–200
- 848 Zook, H. A., Grün, E., Baguhl, M., Hamilton, D. P., Linkert, G., Linkert, D., Liou, J.-C.,
849 Forsyth, R., and Phillips, J. L.: 1996, *Solar wind magnetic field bending of Jovian dust*
850 *trajectories*, *Science* **274**, 1501–1503

Table 1: Summary of Ulysses data papers, significant mission events and dust detector switch-off times. Jupiter distance $R_J = 71492$ km.

Time Interval	Significant Mission Events	Dust Detector off	Paper Number
1990 – 1992	Ulysses launch (6 Oct 1990), Jupiter flyby (8 Feb 1992, distance $6.3 R_J$)	Before 27 Oct 1990, 14 Jun 1991 - 18 Jun 1991	III (Grün et al., 1995a)
1993 – 1995	Maximum southern latitude -79° (3 Oct 1994), Perihelion (12 Mar 1995), Maximum northern latitude 79° (19 Aug 1995)	8 Aug 1993 - 11 Aug 1993, 27 Nov 1993 - 28 Nov 1993, 10 Oct 1994 - 11 Oct 1994, 10 Dec 1995	V (Krüger et al., 1999b)
1996 – 1999	Aphelion (20 Apr 1998),	17 Aug 1996 - 18 Aug 1996, 1 Apr 1997 - 2 Apr 1997, 15 Feb 1999 - 16 Feb 1999	VII (Krüger et al., 2001b)
2000 – 2004	Maximum southern latitude -80° (27 Nov 2000), Perihelion (23 May 2001), Maximum northern latitude 80° (13 Oct 2001), Jupiter flyby (4 Feb 2004, distance 0.8 AU), Aphelion (30 Jun 2004)	26 Mar 2002 - 8 Apr 2002, 1 Dec 2002 - 3 Jun 2003, 28 Jun 2003 - 22 Aug 2003, 30 Nov 2003 - 2 Dec 2003	IX (Krüger et al., 2006a)
2005 – 2007	Maximum southern latitude -80° (7 Feb 2007), Perihelion (18 Aug 2007)	28 Sep 2006 - 9 Mar 2007, 2 Apr 2007 - 30 Apr 2007, After 30 Nov 2007	XI (this paper)

Table 2: Ulysses mission and dust detector (GRU) configuration, tests and other events. Only selected events are given before 2005. See Section 2 for details.

Yr-day	Date	Time	Event
90-279	06.10.90		Ulysses launch
03-154	03.06.03	03:38	GRU 0.8 W heater on
04-182	30.06.04		Ulysses aphelion passage (5.4 AU)
04-337	02.12.04	11:00	GRU nominal configuration: HV=4, EVD=C,I, SSEN=0001
05-006	06.01.05	07:00	GRU noise test
05-034	03.02.05	04:20	GRU noise test
05-063	04.03.05	03:00	GRU noise test
05-090	31.03.05	01:00	GRU noise test
05-120	30.04.05	00:00	GRU noise test
05-146	26.05.05	04:00	GRU noise test
05-174	23.06.05	20:00	GRU noise test
05-201	20.07.05	17:27	GRU noise test
05-229	17.08.05	11:49	GRU noise test
05-259	16.09.05	19:00	GRU noise test
05-285	12.10.05	09:00	GRU noise test
05-314	10.11.05	13:14	GRU noise test
05-342	08.12.05	11:00	GRU noise test
06-005	05.01.06	08:30	GRU noise test
06-033	02.02.06	09:16	GRU noise test
06-061	02.03.06	04:00	GRU noise test
06-089	30.03.06	02:00	GRU noise test
06-118	28.04.06	00:30	GRU noise test
06-148	28.05.06	06:28	GRU noise test
06-173	22.06.06	07:33	GRU noise test
06-202	21.07.06	19:00	GRU noise test
06-232	20.08.06	17:00	GRU noise test
06-256	13.09.06	20:11	GRU noise test
06-271	28.09.06	16:28	GRU off (both heaters off)
07-038	07.02.07		Ulysses maximum south solar latitude (-79.7°)
07-067	08.03.07	18:08	GRU 0.8 W heater on
07-067	08.03.07	18:28	GRU 0.4 W heater on
07-068	09.03.07	16:44	GRU 0.8 W heater off
07-068	09.03.07	17:31	GRU on
07-069	10.03.07	07:54	GRU nominal configuration
07-079	20.03.07	08:40	GRU noise test
07-092	02.04.07	18:11	GRU off (both heaters off)
07-120	30.04.07	01:23	GRU 0.8 W heater on
07-120	30.04.07	01:33	GRU 0.4 W heater on
07-120	30.04.07	21:37	GRU 0.8 W heater off
07-120	30.04.07	21:38	GRU on
07-121	01.05.07	04:07	GRU nominal configuration
07-130	10.05.07	20:00	GRU noise test
07-158	07.06.07	01:00	GRU noise test
07-187	06.07.07	16:15	GRU noise test
07-214	02.08.07	01:53	GRU noise test
07-231	18.08.07		Ulysses perihelion passage (1.39 AU)
07-232	19.08.07		Ulysses ecliptic plane crossing
07-242	30.08.07	00:17	GRU noise test
07-270	27.09.07	17:00	GRU noise test
07-298	25.10.07	13:00	GRU noise test
07-326	22.11.07	15:00	GRU noise test
07-334	30.11.07	16:20	GRU off (both heaters off)
08-014	14.01.08		Ulysses maximum north solar latitude (79.8°)
09-181	30.06.09		Ulysses end of mission

Abbreviations used: HV: channeltron high voltage step; EVD: event definition, ion- (I), channeltron- (C), or electron-channel (E); SSEN: detection thresholds, ICP, CCP, ECP and PCP. Times when no data could be collected with the dust instrument: 28 September 2006 to 9 March 2007, 2 April to 30 April 2007 and after 30 November 2007.

Table 3. Overview of dust impacts detected with the Ulysses dust detector between 1 January 2005 and 30 November 2007 as derived from the accumulators[†]. Switch-on of the instrument is indicated by horizontal lines. The heliocentric distance R , the lengths of the time interval Δt (days) from the previous table entry, and the corresponding numbers of impacts are given for the 24 accumulators. The accumulators are arranged with increasing signal amplitude ranges (AR), with four event classes for each amplitude range (CLN = 0,1,2,3); e.g. AC31 means counter for AR = 1 and CLN = 3. The Δt in the first line (05-006) is the time interval counted from the last entry in Table 2 in Paper IX. The totals of counted impacts[†], of impacts with complete data, and of all events (noise plus impact events) for the entire period are given as well.

Date	Time	R [AU]	Δt [d]	AC 01 [†]	AC 11 [†]	AC 21	AC 31	AC 02 [†]	AC 12	AC 22	AC 32	AC 03	AC 13	AC 23	AC 33	AC 04	AC 14	AC 24	AC 34	AC 05	AC 15	AC 25	AC 35	AC 06	AC 16	AC 26	AC 36
05-006	11:45	5.300	7.561	-	-	-	-	-	-	-	1	-	-	-	-	-	-	-	-	*	-	-	-	*	-	-	-
05-039	23:36	5.258	33.49	-	-	-	2	-	-	5	2	-	-	-	-	-	-	-	-	*	-	-	-	*	-	-	-
05-061	19:36	5.227	21.83	-	3	8	3	-	-	-	2	-	-	-	1	-	-	1	-	*	-	-	-	*	-	-	-
05-089	09:46	5.184	27.59	-	1	11	3	-	-	1	5	2	-	-	-	-	-	-	-	*	-	-	-	*	-	-	-
05-104	17:01	5.158	15.30	-	-	4	2	-	-	-	3	-	-	-	-	-	-	-	1	*	-	-	-	*	-	-	-
05-140	22:27	5.089	36.22	-	5	6	1	-	-	5	2	-	-	-	-	-	-	-	1	*	-	-	-	*	-	-	-
05-177	01:56	5.013	36.14	-	5	4	2	-	-	9	9	-	-	-	-	-	-	-	-	*	-	-	-	*	-	-	-
05-204	13:40	4.949	27.48	-	2	5	1	-	-	2	2	2	-	-	3	-	-	-	-	*	-	-	-	*	-	-	-
05-227	18:13	4.891	23.18	-	4	5	2	-	-	3	7	-	-	-	6	-	-	-	-	*	-	-	-	*	-	-	-
05-250	17:23	4.831	22.96	-	1	6	-	-	-	1	1	7	-	-	2	-	-	-	1	*	-	-	-	*	-	-	-
05-284	14:06	4.734	33.86	-	2	3	-	-	-	2	4	-	-	1	7	-	-	-	-	*	-	-	-	*	-	-	-
05-310	21:37	4.654	26.31	-	1	3	-	-	-	5	5	-	-	-	3	-	-	-	-	*	-	-	-	*	-	-	-
05-337	10:38	4.568	26.54	-	3	-	-	-	-	2	2	-	-	-	1	-	-	-	1	*	-	-	-	*	-	-	-
05-364	06:07	4.475	26.81	-	1	-	-	-	-	1	1	-	-	-	1	-	-	-	-	*	-	-	-	*	-	-	-
06-028	18:17	4.368	29.50	-	2	2	1	-	-	1	3	4	-	-	1	-	-	-	-	*	-	-	-	*	-	-	-
06-052	22:35	4.274	24.17	-	2	3	-	-	-	2	4	-	-	-	2	-	-	-	-	*	-	-	-	*	-	-	-
06-078	05:59	4.172	25.30	-	2	2	-	-	-	1	3	-	-	-	3	-	-	-	-	*	-	-	-	*	-	-	-
06-100	06:53	4.078	22.03	-	-	1	-	-	-	3	1	-	-	1	1	-	-	-	-	*	-	-	-	*	-	-	-
06-132	07:12	3.935	32.01	-	-	2	-	-	-	2	1	-	-	-	5	-	-	-	-	*	-	-	-	*	-	-	-
06-165	22:45	3.776	33.64	-	1	2	1	-	-	1	2	-	-	-	2	-	-	-	1	*	-	-	-	*	-	-	-
06-192	21:07	3.642	26.93	-	-	1	-	-	-	1	1	-	-	-	1	-	-	-	-	*	-	-	-	*	-	-	-
06-217	08:19	3.514	24.46	-	1	1	-	-	-	-	1	-	-	-	1	-	-	-	1	*	-	-	-	*	-	-	-
06-238	08:40	3.400	21.01	-	-	2	-	-	-	-	1	-	-	-	1	-	-	-	-	*	-	-	-	*	-	-	-
06-271	16:30	3.211	33.32	-	-	1	-	-	-	1	2	-	-	-	1	-	-	-	1	*	-	-	-	*	-	-	-
07-069	07:54	2.163	162.6	-	-	-	-	-	-	-	2	-	-	-	-	-	-	-	-	*	-	-	-	*	-	-	-
07-092	18:15	2.004	23.43	-	1	-	-	-	1	2	2	-	-	1	1	-	-	-	-	*	-	-	1	*	-	-	-
07-121	04:07	1.818	28.41	-	-	-	-	-	-	-	1	-	-	-	1	-	-	-	-	*	-	-	-	*	-	-	-
07-152	04:50	1.634	31.02	-	1	6	-	-	1	-	1	-	-	-	2	-	-	1	-	*	-	-	-	*	-	-	-
07-182	21:34	1.489	30.69	-	13	10	4	-	-	-	1	-	-	-	2	-	-	-	-	*	-	-	-	*	-	-	-
07-200	08:56	1.433	17.47	2	12	6	1	-	-	8	5	-	-	-	1	-	-	-	1	*	-	-	-	*	-	-	-
07-222	17:12	1.396	22.34	2	25	17	3	-	1	3	2	-	-	3	-	-	-	1	3	*	-	-	-	*	-	-	-
07-243	23:21	1.402	21.25	3	25	8	1	-	3	9	2	-	-	4	5	-	-	1	2	*	-	2	1	*	-	1	-
07-266	13:56	1.452	22.60	-	5	13	4	-	2	6	2	-	-	4	5	-	-	-	2	*	-	-	-	*	-	-	-
07-288	22:33	1.538	22.35	-	8	9	-	-	1	1	1	-	-	1	2	-	-	-	1	*	-	-	-	*	-	-	-
07-309	22:37	1.644	21.00	-	1	5	-	-	-	2	-	-	-	-	2	-	-	-	2	*	-	-	-	*	-	-	-

Table 3 continued.

Date	Time	R [AU]	Δt [d]	AC 01 [†]	AC 11 [†]	AC 21	AC 31	AC 02 [†]	AC 12	AC 22	AC 32	AC 03	AC 13	AC 23	AC 33	AC 04	AC 14	AC 24	AC 34	AC 05	AC 15	AC 25	AC 35	AC 06	AC 16	AC 26	AC 36	
07-334	16:30	1.790	24.74	-	3	2	-	-	-	-	-	-	-	1	-	-	-	-	-	-	*	-	-	-	*	-	-	-
				7 [†]	131 [†]	159	31	0 [‡]	12	88	76	0	0	17	61	0	0	4	19	*	0	2	2	*	0	1	0	0
				7	131	158	31	0	12	88	76	0	0	17	61	0	0	4	19	*	0	2	2	*	0	1	0	0
				6243	132	159	31	120	12	88	76	2	0	17	61	1	0	4	19	*	0	2	2	*	0	1	0	0

‡: Entries for AC01, AC11 and AC02 are the number of impacts with complete data. Due to the noise contamination of these three categories the number of impacts cannot be determined from the accumulators. The method to separate dust impacts from noise events in these three categories has been given by Baguhl et al. (1993).

*: No entries are given for AC05 and AC06 because they count the overflows of accumulators AC21 and AC31 since the reprogramming in December 2004 (Paper IX).

No.	IMP.DATE	C	AR	S	IA	EA	CA	IT	ET	E	I	E	I	E	I	E	I	E	I	P	E	V	D	P	E	C	C	P	P	HV	R	LON	LAT	D _{up}	ROT	S _{Lon}	S _{Lat}	V	VEF	M	MEF
6711	07-308 19:03	3	4	191	24	28	10	8	6	5	0	1	47	0	1	4	1.63524	351.7	50.9	5.43033	321	151	21	19.5	1.6	7.6·10 ⁻¹²	6.0														
6712	07-309 11:53	3	3	196	23	29	6	5	5	0	1	47	0	1	4	1.63865	351.9	51.2	5.43360	327	145	23	34.6	1.6	9.8·10 ⁻¹³	6.0															
6713	07-309 22:37	2	2	149	10	19	0	8	6	6	0	38	0	1	4	1.64140	352.0	51.5	5.43622	261	204	-8	21.4	1.9	1.5·10 ⁻¹³	10.5															
6714	07-313 19:02	2	1	238	1	1	0	15	15	12	0	2	31	1	4	1.66299	353.1	53.5	5.45691	23	84	26	11.8	11.8	1.9·10 ⁻¹⁴	5858.3															
6715	07-315 23:14	2	1	62	7	11	0	8	7	7	0	3	31	1	4	1.67505	353.8	54.5	5.46850	134	344	-26	34.6	1.6	7.6·10 ⁻¹⁵	6.0															
6716	07-322 23:06	1	1	152	4	3	0	9	15	0	1	2	24	1	4	1.71586	356.0	57.9	5.50781	255	211	-11	14.1	1.9	2.8·10 ⁻¹⁴	10.5															
6717	07-327 11:18	1	1	181	5	7	0	9	15	0	1	2	24	1	4	1.74286	357.7	59.9	5.53397	293	181	8	5.7	2.1	7.9·10 ⁻¹³	15.7															
6718	07-327 23:30	1	1	150	2	9	0	9	15	0	1	60	37	31	1	1.74589	357.8	60.1	5.53692	249	218	-14	11.8	11.8	8.8·10 ⁻¹⁴	5858.3															
6719	07-334 08:17	2	3	151	19	7	1	7	15	0	1	46	31	1	4	1.78513	0.4	62.9	5.57519	246	223	-16	14.1	1.9	4.3·10 ⁻¹³	10.5															

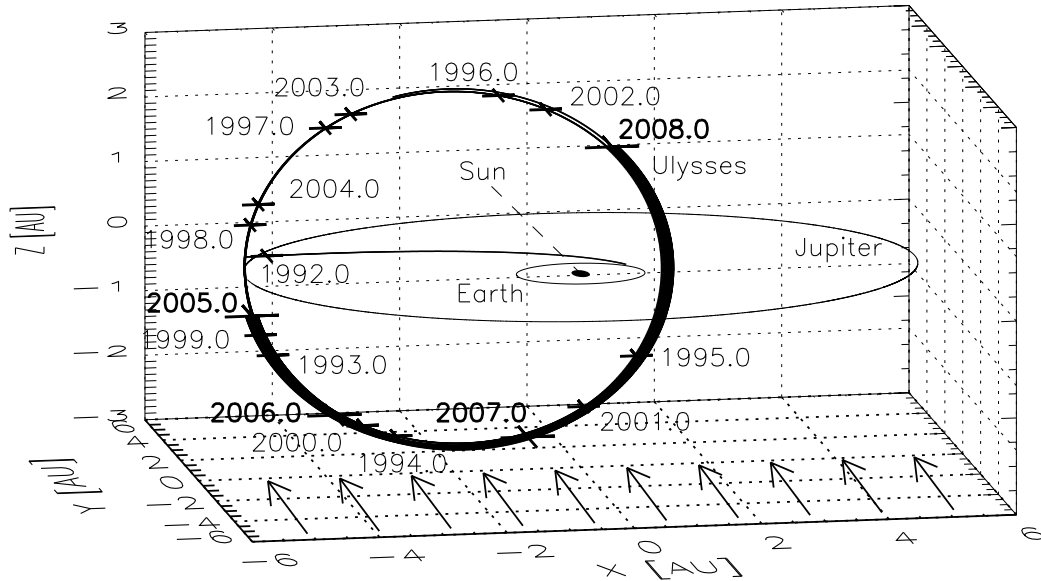


Figure 1: The trajectory of Ulysses in ecliptic coordinates with the Sun at the centre. The orbits of Earth and Jupiter indicate the ecliptic plane, and the initial trajectory of Ulysses was in this plane. Since Jupiter flyby in early 1992 the orbit has been almost perpendicular to the ecliptic plane (79° inclination). Crosses mark the spacecraft position at the beginning of each year. The 2005 to 2007 part of the trajectory is shown as a thick line. Vernal equinox is to the right (positive x axis). Arrows indicate the undisturbed interstellar dust flow direction which is within the measurement accuracy co-aligned with the direction of the interstellar helium gas flow. It is almost perpendicular to the orbital plane of Ulysses.

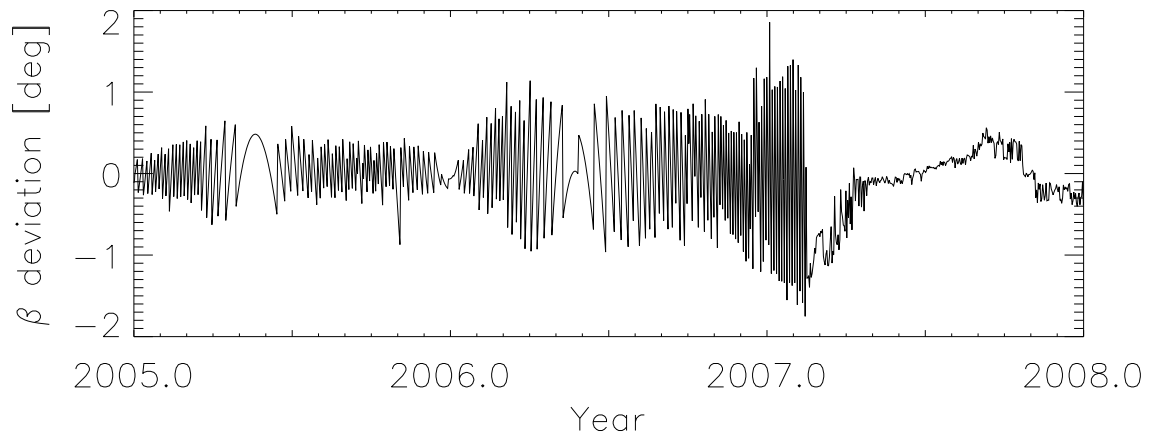
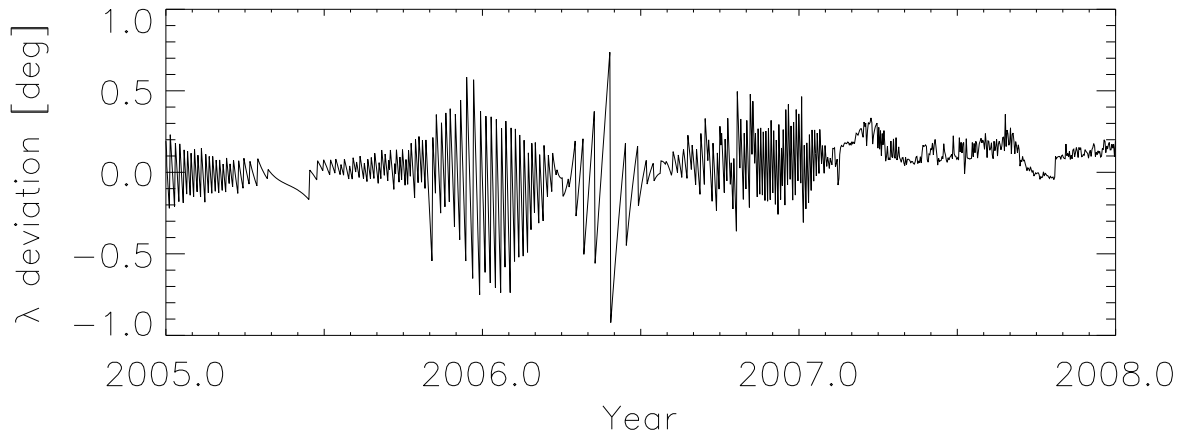


Figure 2: Spacecraft attitude: deviation of the antenna pointing direction (i.e. positive spin axis) from the nominal Earth direction. The angles are given in ecliptic longitude (top) and latitude (bottom, equinox 1950.0).

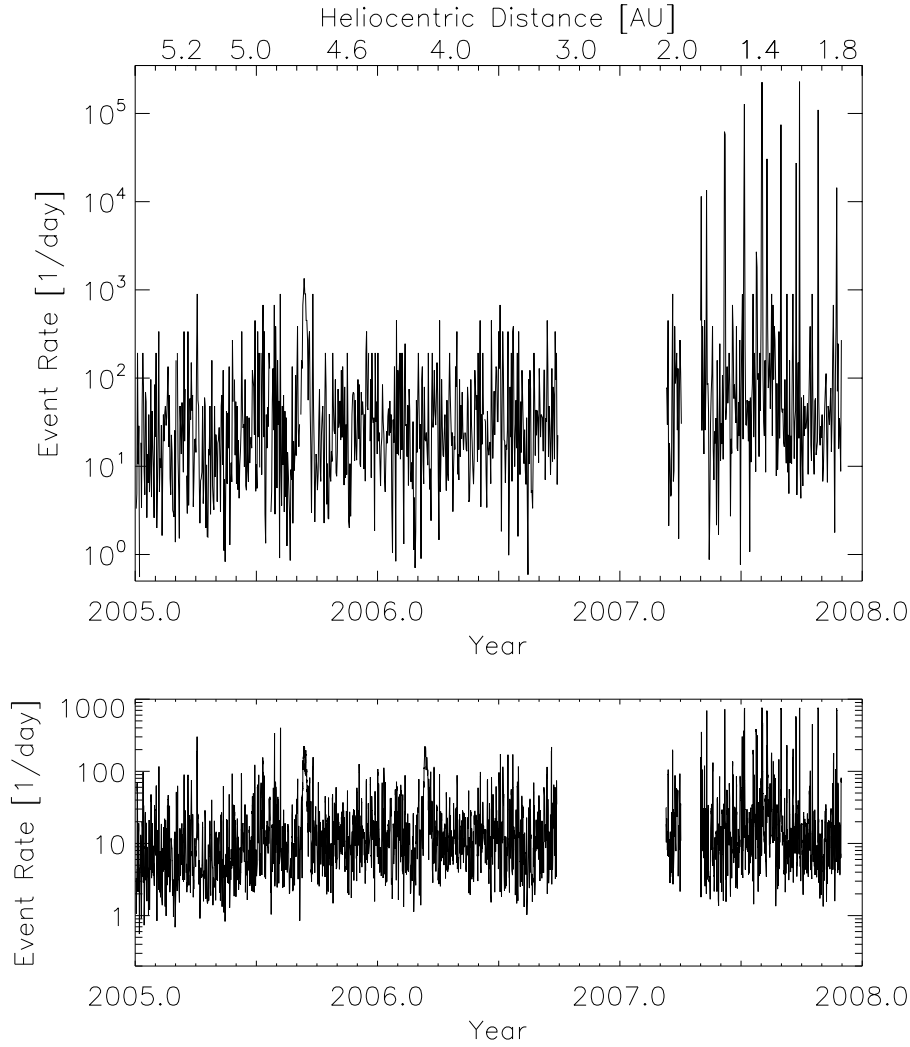


Figure 3: Noise rate (class 0 events) detected with the dust instrument. The heliocentric distance of Ulysses is indicated at the top. Upper panel: Daily maxima in the noise rate (determined from the AC01 accumulator). Sharp spikes which are strongest after May 2008 when Ulysses was in the inner solar system are caused by periodic noise tests. Lower panel: One-day average of the noise rate calculated from the number of AC01 events for which the complete information was transmitted to Earth.

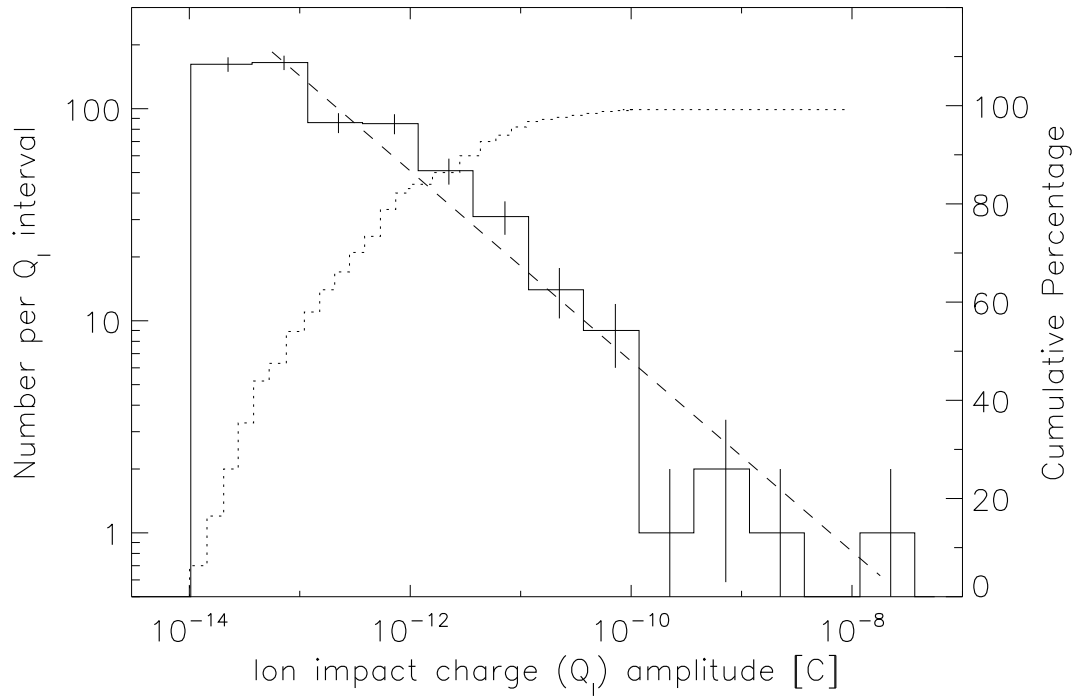


Figure 4: Distribution of the impact charge amplitude Q_I for all dust particles detected from 2005 to 2007. The solid line indicates the number of impacts per charge interval, and the dotted line shows the cumulative percentage. Vertical bars indicate the \sqrt{n} statistical fluctuation. A power law fit to the data with $Q_I > 3 \cdot 10^{-14} \text{ C}$ is shown as a dashed line (Number $N \sim Q_I^{-0.45}$).

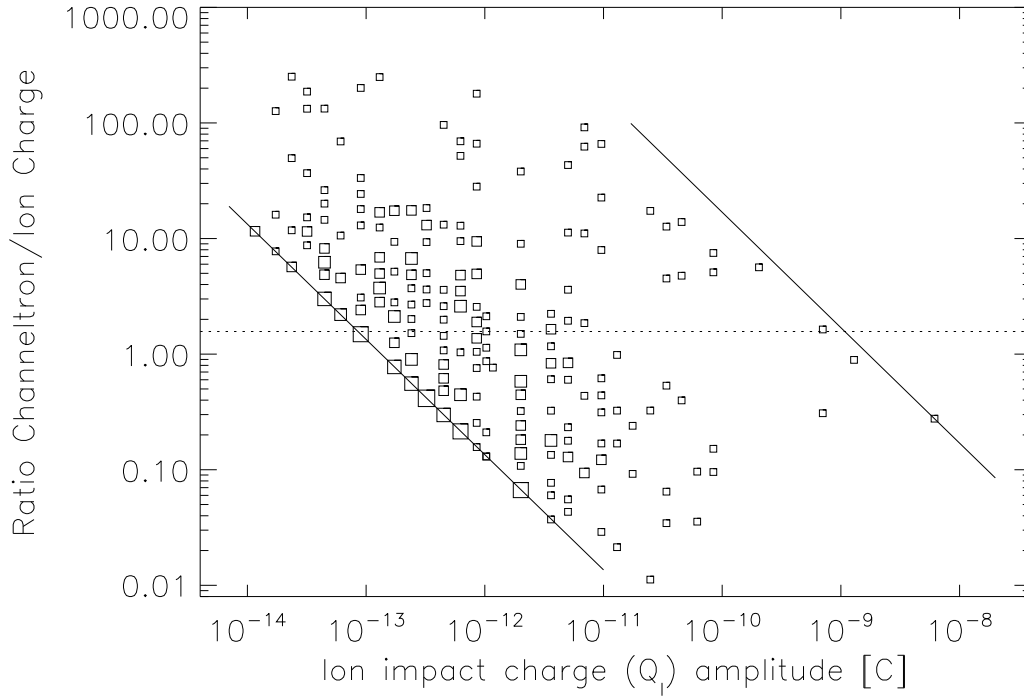


Figure 5: Channeltron amplification factor $A = Q_C/Q_I$ as a function of impact charge Q_I for all dust impacts detected between 2005 and 2007 with channeltron voltage set to HV = 4. The solid lines denote the sensitivity threshold (lower left) and the saturation limit (upper right) of the channeltron. Squares indicate dust particle impacts. The area of each square is proportional to the number of events included (the scaling of the squares is not the same as in earlier papers). The dotted horizontal line shows the mean value of the channeltron amplification $A = 1.57$ for ion impact charges $10^{-12} \text{ C} < Q_I < 10^{-11} \text{ C}$ (82 particles).

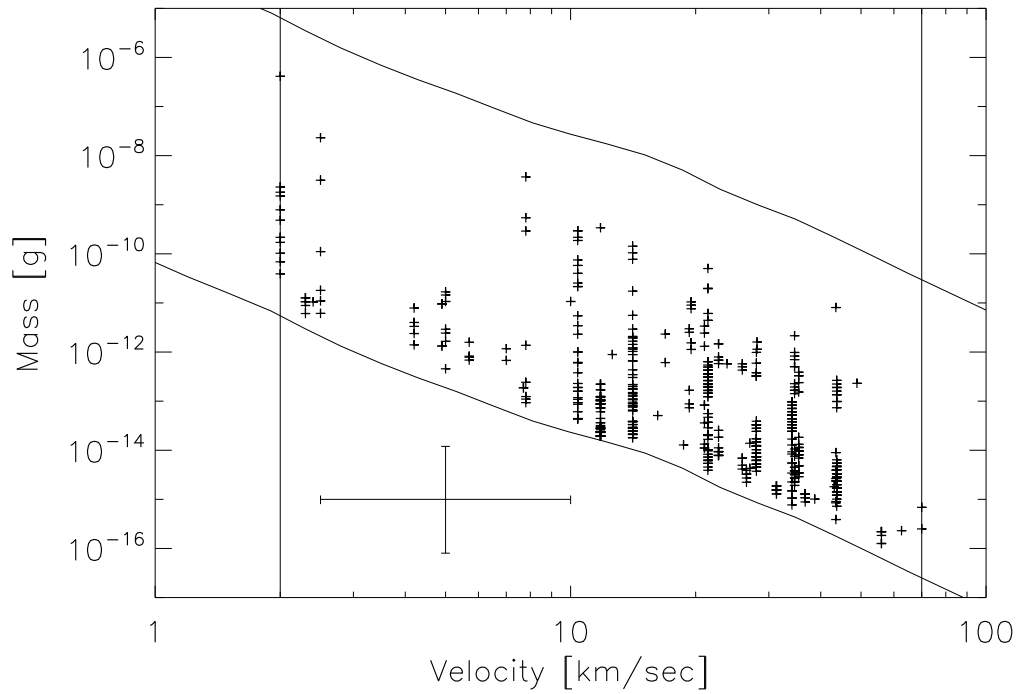


Figure 6: Masses and impact velocities of all impacts recorded with the Ulysses sensor from 2005 to 2007. The lower and upper solid lines indicate the threshold and the saturation limit of the detector, respectively, and the vertical lines indicate the calibrated velocity range. A sample error bar is shown that indicates a factor of 2 uncertainty for the velocity and a factor of 10 for the mass determination.

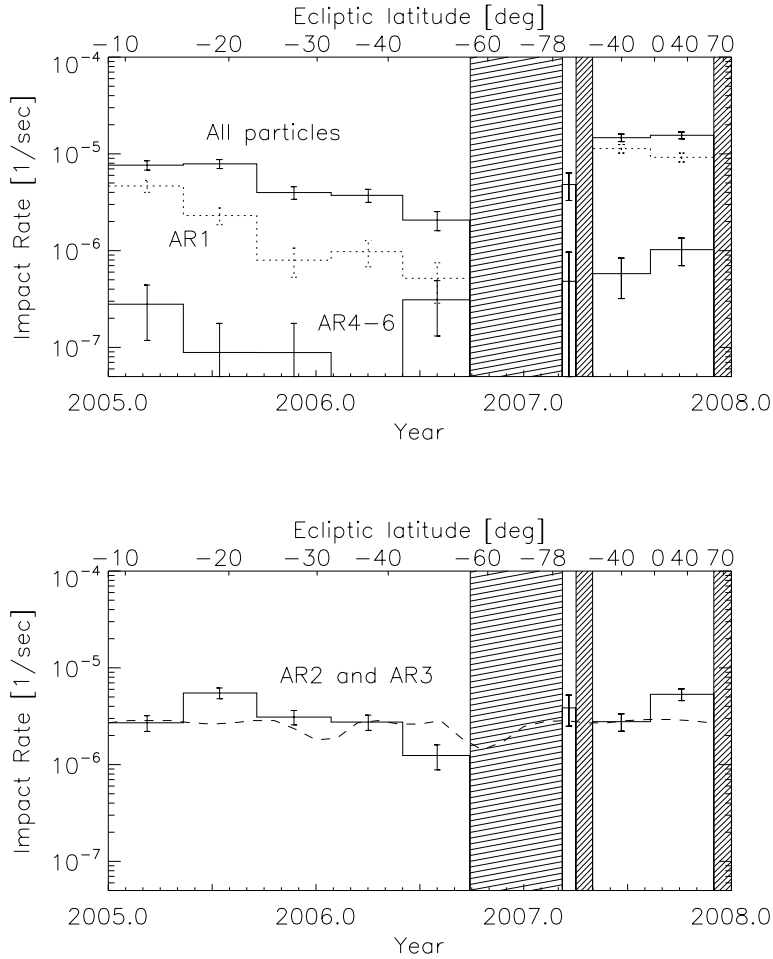


Figure 7: Impact rate of dust particles detected with the Ulysses dust sensor as a function of time. The ecliptic latitude of the spacecraft is indicated at the top. Shaded areas indicate periods when the dust instrument was switched off. Upper panel: total impact rate (upper solid histogram), impact rate of small particles (AR1, dotted histogram), and impact rate of big particles (AR4 – AR6, lower solid histogram). Note that a rate of about 10^{-7} impacts per second is caused by a single dust impact in the averaging interval of about 130 days. An averaging interval of only 24 days had to be used for March 2007 because the instrument was switched off before and after this period. Lower panel: impact rate of intermediate size particles (AR2 and AR3, solid histogram). A model for the rate of interstellar particles assuming a constant flux was fit to the data and is superimposed as a dashed line. Vertical bars indicate the \sqrt{n} statistical fluctuation.

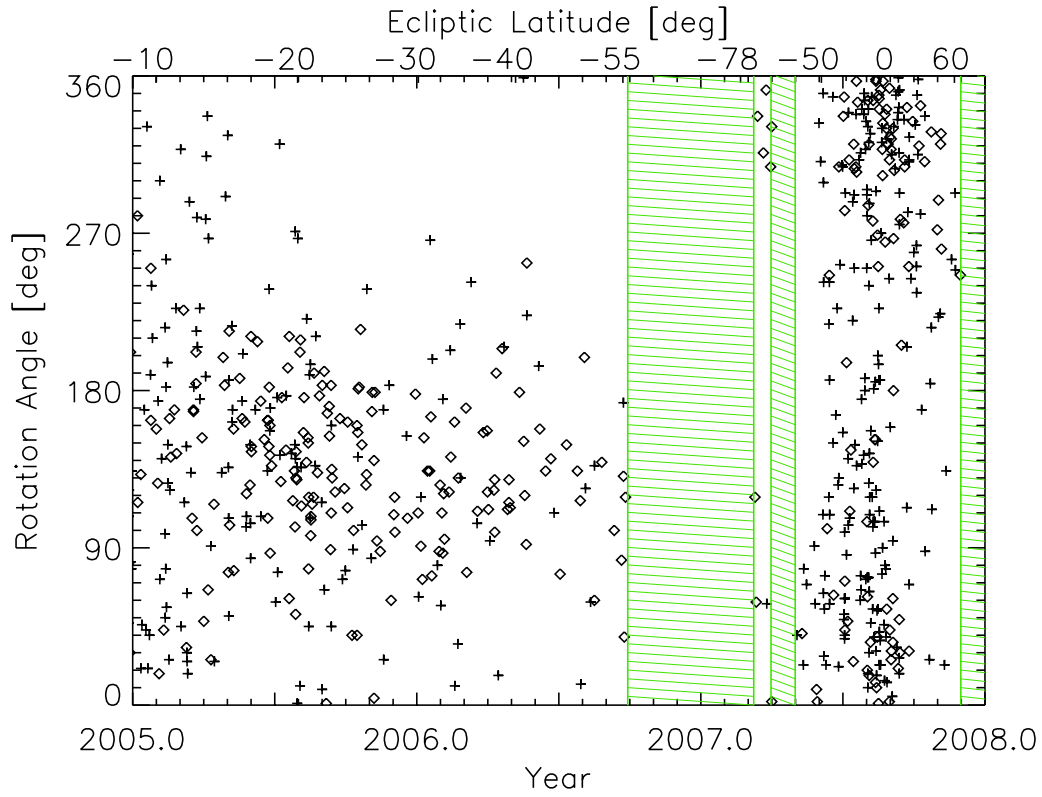


Figure 8: Rotation angle vs. time for all particles detected in the 2005-07 interval. Plus signs indicate particles with impact charge $Q_I < 10^{-13}$ C (AR1), diamonds those with $Q_I > 10^{-13}$ C (AR2 to AR6). Ulysses' ecliptic latitude is indicated at the top.

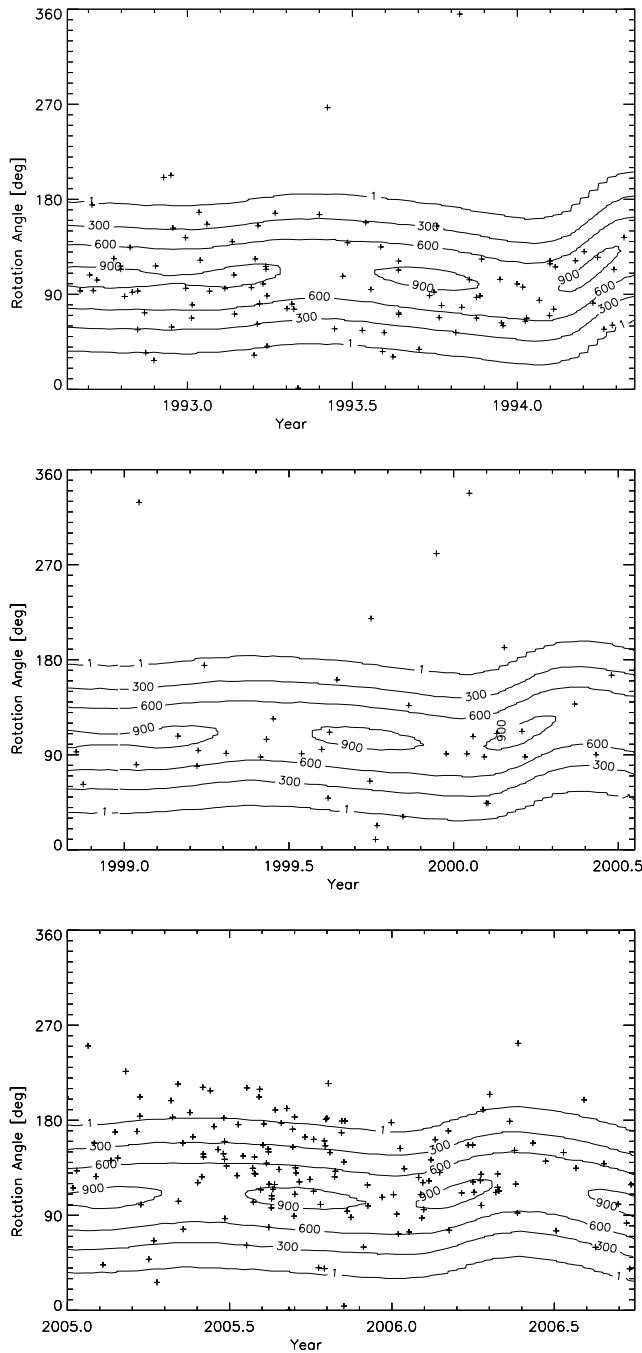


Figure 9: Rotation angle vs. time for dust impacts detected during three time intervals when Ulysses was traversing the same portion of its trajectory between -8.5° and -56° ecliptic latitude. Contour lines show the effective sensor area for dust particles approaching from the upstream direction of interstellar helium (Witte, 2004; Witte et al., 2004). Here we show particles with impact charges $1.5 \cdot 10^{-13} \text{ C} < Q_I < 10^{-11} \text{ C}$ which approximately coincides with AR2-3.

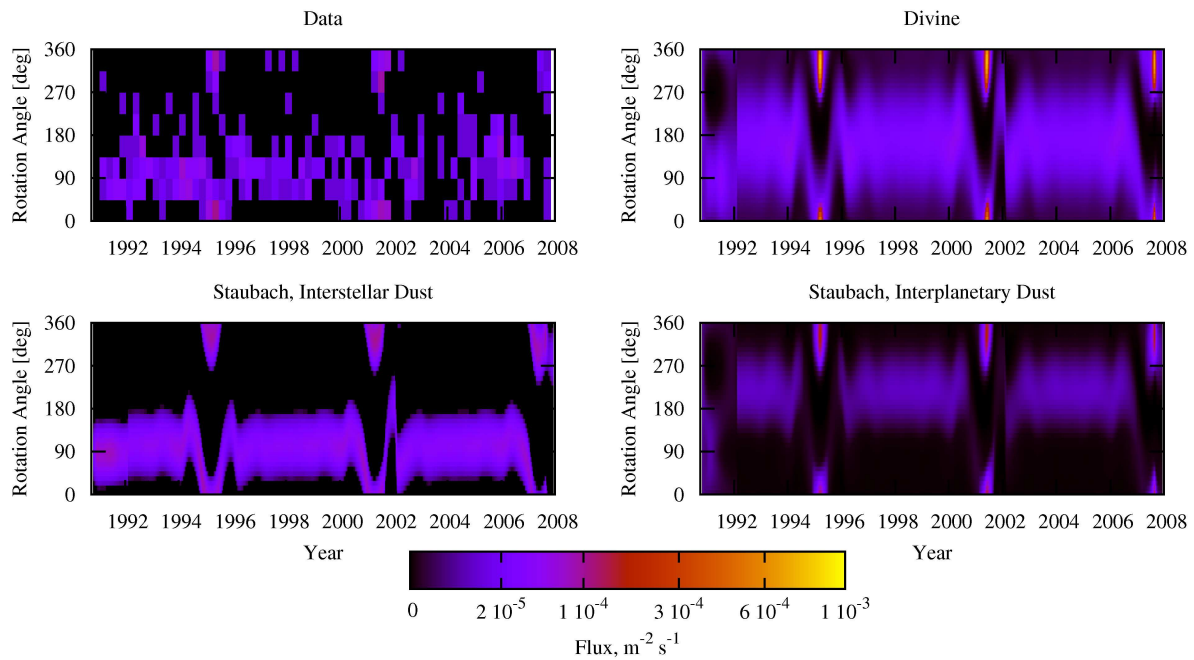


Figure 10: Particle fluxes onto the Ulysses dust detector as seen in the data (AR3 to AR6) and predicted by the meteoroid environment models by Divine (1993) and Staubach et al. (1997). The Jupiter encounter in 1992 is best seen on the model plots as a sharp swing in directionality of impacts caused by the rotation of spacecraft velocity relative to the giant planet. The ecliptic plane crossings near the perihelia in 1995, 2001 and 2007 are marked by the high impact rates due to the number density of dust increase near the Sun and high speed of Ulysses relative to this dust. As the spacecraft moved north at the times of the crossings, the meteoroids came from the ecliptic north as well (rotation angle 0).